
Evaluation and Acceptance of Welded and Repair-Welded Stainless Steel for LWR Service

Annual Report for 1983

Prepared by D. G. Atteridge, S. M. Bruemmer, R. E. Page

Pacific Northwest Laboratory
Operated by
Battelle Memorial Institute

Prepared for
U.S. Nuclear Regulatory
Commission

NOTICE

This report was prepared as an account of work sponsored by an agency of the United States Government. Neither the United States Government nor any agency thereof, or any of their employees, makes any warranty, expressed or implied, or assumes any legal liability of responsibility for any third party's use, or the results of such use, of any information, apparatus, product or process disclosed in this report, or represents that its use by such third party would not infringe privately owned rights.

NOTICE

Availability of Reference Materials Cited in NRC Publications

Most documents cited in NRC publications will be available from one of the following sources:

1. The NRC Public Document Room, 1717 H Street, N.W.
Washington, DC 20555
2. The NRC/GPO Sales Program, U.S. Nuclear Regulatory Commission,
Washington, DC 20555
3. The National Technical Information Service, Springfield, VA 22161

Although the listing that follows represents the majority of documents cited in NRC publications, it is not intended to be exhaustive.

Referenced documents available for inspection and copying for a fee from the NRC Public Document Room include NRC correspondence and internal NRC memoranda; NRC Office of Inspection and Enforcement bulletins, circulars, information notices, inspection and investigation notices; Licensee Event Reports; vendor reports and correspondence; Commission papers; and applicant and licensee documents and correspondence.

The following documents in the NUREG series are available for purchase from the NRC/GPO Sales Program: formal NRC staff and contractor reports, NRC-sponsored conference proceedings, and NRC booklets and brochures. Also available are Regulatory Guides, NRC regulations in the *Code of Federal Regulations*, and *Nuclear Regulatory Commission Issuances*.

Documents available from the National Technical Information Service include NUREG series reports and technical reports prepared by other federal agencies and reports prepared by the Atomic Energy Commission, forerunner agency to the Nuclear Regulatory Commission.

Documents available from public and special technical libraries include all open literature items, such as books, journal and periodical articles, and transactions. *Federal Register* notices, federal and state legislation, and congressional reports can usually be obtained from these libraries.

Documents such as theses, dissertations, foreign reports and translations, and non-NRC conference proceedings are available for purchase from the organization sponsoring the publication cited.

Single copies of NRC draft reports are available free, to the extent of supply, upon written request to the Division of Technical Information and Document Control, U.S. Nuclear Regulatory Commission, Washington, DC 20555.

Copies of industry codes and standards used in a substantive manner in the NRC regulatory process are maintained at the NRC Library, 7920 Norfolk Avenue, Bethesda, Maryland, and are available there for reference use by the public. Codes and standards are usually copyrighted and may be purchased from the originating organization or, if they are American National Standards, from the American National Standards Institute, 1430 Broadway, New York, NY 10018.

\$4.50

GPO Printed copy price: _____

Evaluation and Acceptance of Welded and Repair-Welded Stainless Steel for LWR Service

Annual Report for 1983

Manuscript Completed: September 1983
Date Published: June 1984

Prepared by
D. G. Atteridge, S. M. Bruemmer, R. E. Page

Pacific Northwest Laboratory
Richland, WA 99352

Prepared for
Division of Engineering Technology
Office of Nuclear Regulatory Research
U.S. Nuclear Regulatory Commission
Washington, D.C. 20555
NRC FIN B2449

ABSTRACT

Pacific Northwest Laboratory (PNL), under a program sponsored by the Division of Engineering Technology of the U.S. Nuclear Regulatory Commission (NRC), is conducting a program to determine a method for evaluating the acceptance of welded and repair-welded stainless steel (SS) piping for light-water reactor (LWR) service. Validated models, based on experimental data, will be developed to predict the degree of sensitization (DOS) and the intergranular stress corrosion cracking (IGSCC) susceptibility in the heat-affected zone (HAZ) of the SS weldments. IGSCC is caused by a combination of a sensitized microstructure, an aggressive environment, and tensile stress. Control of any of these three factors can eliminate IGSCC in most practical situations.

This program will measure and model the development of a sensitized microstructure as it pertains to welded and repair-welded SS pipe. An empirical correlation between a material's DOS and its susceptibility to IGSCC will be determined using constant extension rate tests (CERTs). The successful completion of these tasks will result in a method for assessing the effects of welding/repairing parameters on the IGSCC susceptibility of component-specific nuclear reactor welds/repairs.

The present report describes the progress of these studies during the 1983 fiscal year.

SUMMARY

Pacific Northwest Laboratories (PNL), under a program sponsored by the Division of Engineering Technology of the U.S. Nuclear Regulatory Commission (NRC), is conducting a program to determine a method for evaluating the acceptance of welded and repair-welded stainless steel (SS) piping for light-water reactor (LWR) service. Validated models, based on experimental data, will be developed to predict the degree of sensitization (DOS) and the intergranular stress corrosion cracking (IGSCC) susceptibility in the heat-affected zone (HAZ) of the SS weldments. IGSCC is caused by a combination of a sensitized microstructure, an aggressive environment, and tensile stress. Control of any of these three factors can eliminate IGSCC in most practical situations.

This program will measure and model the development of a sensitized microstructure as it pertains to welded and repair-welded SS pipe. An empirical correlation between a material's DOS and its susceptibility to IGSCC will be determined using constant extension rate tests (CERTs). The successful completion of these tasks will result in a method for assessing the effects of welding/repairing parameters on the IGSCC susceptibility of component-specific nuclear reactor welds/repairs.

This report describes the initial efforts needed to develop the data base for this study. A measurement system capable of measuring temperatures and strains in the HAZ on the inside surface of SS pipe welds was developed. A data retrieval and analysis system capable of recording the resultant thermomechanical histories was designed, and assembly was initiated.

It was determined that the electrochemical potentiokinetic reactivation (EPR) test would be the primary method used to measure DOS values. Equipment for standard laboratory and for field work was obtained and calibrated. The standard cell equipment was used to determine DOS histories on a series of furnace-treated Type 304 SS heats as a function of carbon content. Field polishing techniques were developed for use with the field cell, and a method to decrease the field cell probe size was developed. The field cell was calibrated against the standard laboratory cell and was used to measure DOS profiles on a 24-in.-dia. Type 304 SS weldment as a function of probe size. The subsized field probe yielded a distinctly different DOS profile than the standard field cell probe due to the averaging effect of the larger probe.

Initial predictive calculations were begun for predicting the effect of material composition on IGSCC susceptibility. The calculations were based on existing models and the results were compared to the experimentally determined DOS changes as a function of composition. The current models were found to predict the change in maximum DOS values fairly well, but could not be used to predict intermediate DOS values.

CONTENTS

ABSTRACT.....	iii
SUMMARY.....	v
INTRODUCTION	1
TASK I: WELD THERMOMECHANICAL HISTORY DETERMINATION.....	3
DATA RETRIEVAL AND ANALYSIS SYSTEM.....	4
Data Storage and Retrieval.....	4
Signal Retrieval, Isolation, and Conditioning.....	4
Signal Generation.....	5
INSTRUMENT DOMAIN.....	5
STRAIN MEASUREMENT DEVICE.....	7
FLAT PLATE FEASIBILITY WELD.....	11
INTERACTIONS WITH OTHER LABORATORIES.....	23
TASK II. INFLUENCE OF COMPOSITION AND THERMOMECHANICAL HISTORY ON DOS AND IGSCC.....	25
DEGREE OF SENSITIZATION MEASUREMENT.....	25
STRESS CORROSION CRACKING SUSCEPTIBILITY MEASUREMENT.....	30
COMPOSITION EFFECTS ON SENSITIZATION: CARBON SERIES.....	30
INTERACTIONS WITH OTHER LABORATORIES.....	35
TASK III: IGSCC PREDICTION METHODOLOGY FROM COMPONENT-SPECIFIC THERMOMECHANICAL HISTORIES.....	39
DEGREE OF SENSITIZATION PREDICTION: EFFECT OF COMPOSITION.....	39
DEGREE OF SENSITIZATION PREDICTION: KINETICS OF CHROMIUM DEPLETION.....	42
INTERACTIONS WITH OTHER LABORATORIES.....	42
FUTURE RESEARCH PLANS.....	44
REFERENCES.....	45

FIGURES

1	Data Retrieval and Analysis System.....	4
2	Calibration of a Clip Gage.....	6
3	Schematic of the Profilometer Used to Measure Strain Perpendicular to the Plate Surface.....	6
4	Profilometer Unit Attached to a Flat Plate.....	7
5	Instrument Domain Layout.....	8
6	Instrument Domain Showin Thermocouple and Surface Movement Marker Layout.....	9
7	Profilometer Unit, Surface Movement Clip Gages, and Thermocouples Attached to the Flat Plate Feasibility Weld.....	9
8	Instrument Domain Showing Profilometer Superimposed over Thermocouple and Surface Movement Marker Layout.....	10
9	MTS Strain Sensing Units Adapted for High-Temperature Use.....	11
10	HAZ Surface Profiles After Initial Temperature Rise.....	12
11	Two-Dimensional Surface Thermal Profile Around Arc.....	13
12	Flat Plate Weld Surface Temperature Gradient.....	14
13	Surface Strain Parallel to Welding Direction, and Temperature 0.2 in. from Weld Centerline.....	16
14	Surface Strain Parallel to Welding Direction, and Temperature 0.4 in. from Weld Centerline.....	16
15	Surface Strain Perpendicular to Welding Direction, and Temperature 0.4 in. from Weld Centerline.....	17
16	Surface Strain Perpendicular to Welding Direction, and Temperature 0.6 in. from Weld Centerline.....	17
17	Surface Strain Parallel to Welding Direction, and Temperature 0.8 in. from Weld Centerline.....	18
18	Comparison of Strain Changes During Welding as a Function of Distance from the Fusion Line and Direction of Strain.....	18
19	Strain Measurements from Gages Parallel to Welding Direction.....	19

20	Strain Measurements from Gages Perpendicular to Welding Direction.....	19
21	Surface Movement Perpendicular to Plate Surface at Weld Centerline.....	20
22	Thermal Bump Displacement as a Function of Distance from the Weld Centerline.....	20
23	Thermal Bump Height as a Function of Distance from the Weld Centerline.....	21
24	Three Dimensional Representation of the Thermal Bump Induced at the Plate Surface During Welding.....	21
25	Surface Movement 0.4 in. from the Fusion Line in the x, y, and z Directions Correlated with the Weld-Induced Change in Temperature.....	22
26	EPR Measurements on a Severely Sensitized Type 304 SS Specimen as a Function of Test Solution Temperature.....	26
27	Change in EPR Measurement as a Function of Surface Activation Treatment Time.....	28
28	Surface Appearance After a Standard and an Activated Test on a Furnace-Sensitized Type 304L SS.....	29
29	Degree of Sensitization Measurements as a Function of Distance from the Weld Fusion Line for Three Probe Sizes.....	31
30	EPR Values as a Function of Isothermal Annealing Time for Three Type 304 SS Alloys of Differing Carbon Levels.....	33
31	Scanning Electron Micrographs of Typical Surface Conditions after EPR Testing of Furnace-Sensitized Type 304 SS.....	34
32	Intergranular Carbide Distributions in Four Carbon Series (Type 304 SS) Alloys After a 625°C Heat Treatment for 24 h.....	36
33	Comparison of Chromium Depletion Measured by STEM-EDS and by EPR on Furnace-Sensitized Type 304 SS Alloys.....	37
34	Cihal Plot Indicating Relative IGSCC Susceptibility for Carbon Series Alloys.....	41
35	Comparison of EPR-Measured Degree of Sensitization to the Predicted Composite Chromium Content from Composition Models; 625°C for 24 h.....	43

36	Comparison of EPR-Measured Degree of Sensitization to the Predicted Composite Chromium Contents from Composition Models; 700°C for 10 h.....	43
37	Correlation Between the EPR-Measured Degree of Sensitization and the Predicted Width of the Chromium-Depleted Region at Grain Boundaries as a Function of Heat Treatment Time at 700°C.....	44

TABLES

1	Composition of Carbon Series Alloys.....	27
2	Comparison of Field and Laboratory Cell EPR Tests on Furnace-Sensitized Type 304 SS.....	30
3	Heat Treatment Matrix for Isothermal Testing of Carbon Series Alloys.....	32
4	TVA Material Selection.....	38
5	Comparison of Model Predictions for Chromium Equivalent Parameters of Carbon Series Alloys.....	42

INTRODUCTION

In 1981, Pacific Northwest Laboratory (PNL)^(a) and the Division of Engineering Technology of the U.S. Nuclear Regulatory Commission (NRC) began a program to determine a method for evaluating the acceptance of welded and repair-welded stainless steel (SS) piping for light-water reactor (LWR) service. Validated models, based on experimental data, will be developed to predict the degree of sensitization (DOS) and the intergranular stress corrosion cracking (IGSCC) susceptibility in the heat-affected zone (HAZ) of the SS weldments. The cumulative effects of material composition, past fabrication procedures, past service exposure, weldment thermomechanical (TM) history, and projected post-repair component life will be considered.

Austenitic SS components of commercial boiling-water (BWR) and pressurized water (PWR) reactors have experienced IGSCC in the HAZ of in-service SS welds. Although only a few instances of such cracking have been observed, their potential for causing serious component failure should not be underestimated. IGSCC is caused by a combination of a sensitized microstructure, an aggressive environment, and tensile stress. Control of any of these three factors can eliminate IGSCC in most practical situations.

This program will measure and model the development of a sensitized microstructure as it pertains to welded and repair-welded SS pipe. An empirical correlation between a material's DOS and its susceptibility to IGSCC will be determined using constant extension rate tests (CERTs). The successful completion of these tasks will result in a method for assessing the effects of welding/repairing parameters on the IGSCC susceptibility of component-specific nuclear reactor welds/repairs.

Component-specific determinations of DOS and IGSCC susceptibility for HAZs after welding/repairing will require a practical method for determining the fabrication history of the components. This program will use component-specific mill heat chemistries, in addition to the processing and fabrication records already required in the nuclear industry, for initial DOS predictions. Recommendations for increased procedure controls and record changes will be made as required to attain realistic DOS predictions.

The test matrix will include various Type 304, 304L, 304NG, 316, 316L and 316NG SS materials used in nuclear reactor piping systems. The proposed program plan consists of the following phases:

Task I: Weld Thermomechanical History Determination

- experimental determination of the TM history of the HAZ on the pipe interior during primary and repair welds

(a) Operated for the U.S. Department of Energy (DOE) by Battelle Memorial Institute.

- experimental determination of the DOS and IGSCC susceptibility of fully characterized pipe welds and subsequent repair welds.

Task II: Influence of Composition and Thermomechanical History on DOS and IGSCC

- experimental determination of the effects of bulk material composition on HAZ, DOS and IGSCC susceptibility
- experimental assessment of the DOS and IGSCC susceptibility of comparable weldments fabricated using machine and manual welding techniques.

Task III: IGSCC Prediction Methodology from Component-Specific Thermomechanical Histories

- development of a HAZ TM history prediction method
- development of a HAZ DOS prediction method
- experimental and modeling efforts needed to determine the relationship between a given weld-induced DOS and its susceptibility to IGSCC
- development of a practical method for assessing the IGSCC susceptibility of the HAZ of component-specific welds/repairs.

The progress achieved toward these goals in FY 1983, including the results of the initial testing and cooperative work with other laboratories, is presented in the following sections.

TASK I: WELD THERMOMECHANICAL HISTORY DETERMINATION

A weld/repair HAZ is subject to a complicated strain history superimposed over the heating and cooling cycle. Recent work indicates that this strain cycle increases the resultant sensitization of the HAZ over that predicted from strain-free isothermal data or that measured in specimens subjected to a similar but strain-free heating and cooling cycle. It is therefore necessary to precisely determine the strain/temperature history of a HAZ. The HAZ strain history is more complex in a multipass weld/repair than in a single pass weld/repair. Strain history is also more complex in a pipe weld/repair than in a plate weld/repair; stresses can be relieved by plate bending, while circumferential restraint restricts metal movement in a pipe weld.

Previous experimentation involving the HAZ TM history concentrated on temperature measurements as a function of time and distance from the fusion line. The present work will determine simultaneously the strain and temperature history in welded/repared pipe HAZs as a function of time and distance from the fusion line. It is expected that the resultant HAZ TM history will be a complex function of system restraint and heat absorption capability. Variables that can be expected to influence the TM history are pipe diameter and wall thickness, changes in wall thickness from one side of the fusion line to the other, depth of counterbore, weld/repair groove geometry, amount of weld crowning, weld heat input, length and depth of repair, and welding technique.

A major goal of this task is to identify and measure the welding and repair-welding variables that have a major effect on resultant DOS, and to assess the ability to predict HAZ TM histories analytically. The initial work will be oriented toward experimentally determining HAZ TM histories of welds/repairs as a function of pipe size and heat input. These data will then be used to assess analytical methods for predicting TM histories of generic welds/repairs and the effect of specific welding and repair-welding variables on the resultant TM history.

The focus of the current experimental work is on the TM history of a thin layer on the inside surface of the pipe, as it is this region that controls IGSCC initiation. The placement of strain measurement devices and thermocouples on the pipe surface will allow real-time TM history measurement.

The decision to measure TM histories dictated the need for fast response signal recording capabilities, strain measurement devices that can withstand temperatures up to the melting point of stainless steels, and signal generation equipment that can withstand an electric welding arc superimposed over the desired strain or temperature measurement device signal. The resultant data must also be deciphered once the test is complete; thus, a Data Retrieval and Analysis System (DRAS) is being developed specifically for this program.

DATA RETRIEVAL AND ANALYSIS SYSTEM

The DRAS is composed of several components, including: 1) data storage and retrieval; 2) signal receiving, isolation and conditioning; and 3) signal generating. These are schematically illustrated in Figure 1.

Data Storage and Retrieval

A Data General Nova computer is the heart of the data storage and computation segment of the DRAS. The computer has a high data rate analog-to-digital (A-to-D) conversion front end and access to graphics printing equipment. It is equipped with a fast data storage and retrieval hard disk drive unit as well as a magnetic tape data storage and retrieval unit. The latter was added to allow transfer of the experimental data to a computer capable of comparing TM histories predicted by finite element modeling with actual experimental data. The Nova computer is being programmed to accept multiple input signals from the A-to-D converter.

Signal Retrieval, Isolation, and Conditioning

The signal retrieval, isolation, and conditioning segments of the DRAS consist of multiple independent input channels. Signal filtering units are in series with signal isolation and signal amplification units. The first two units remove the arc noise from the incoming signal and ensure that the arc current is not passed into the amplification units. The amplification units raise the signal voltage to the correct level for the A-to-D converter.

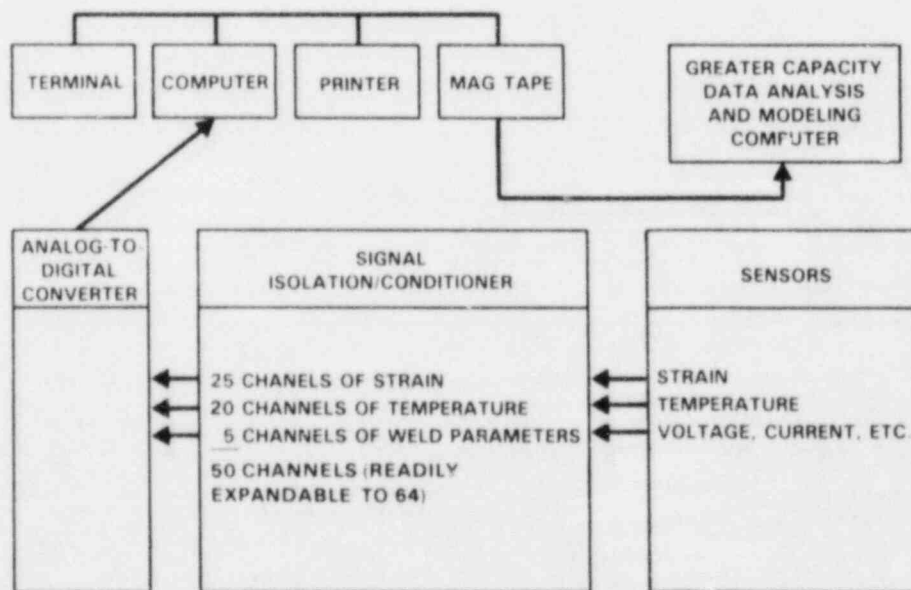


FIGURE 1. Data Retrieval and Analysis System

Signal Generation

The signal generating segment of the DRAS consists of sensors that detect changes in strain, temperature, and welding parameters. Each of these sensors requires different filtering and amplification. Multiple combinations of filter levels and amplifier types have been tested for the various input signals present during actual welding conditions. A compatible series of filtering, isolation, and amplification units have been determined for each signal type and are now being hard-wired into a signal conditioning instrument rack.

The temperature measurement sensors are conventional thermocouples and the welding parameters are picked up from the welding controller weld parameter gages. No commercially available strain sensors could withstand temperatures up to the melting point of stainless steel or multiple plastic strain cycles; thus, strain measurement sensors have been designed specially for this program.

Two types of strain sensors have been developed. The first type senses strain changes parallel to the pipe surface, while the second senses strain changes perpendicular to the pipe surface. The parallel strain sensors consist of three separate parts. A set of surface movement markers is attached directly to the pipe surface in order to detect relative movement between the positions of the two markers. A set of ceramic stand-off legs is attached to the surface movement markers to insulate the strain gages from the temperatures to which the surface markers are exposed. A full bridge strain-gaged clip gage is attached to the ceramic legs. The clip gage comprises two strain-gaged arms separated by a rectangular spacer at one end and connected to the ceramic arms at the other end. A strain sensor unit attached to surface markers that are welded to the sensor calibration micrometer is shown in Figure 2.

The perpendicular strain measurement device is referenced to a line that is parallel to the pipe's inside surface but above the weld zone (counterbore region). This is done by attaching a "bridge" to the inside pipe surface beyond the counterbore region on both sides of the weld. Ceramic pins, dropped from this reference line, rest in indentations in the pipe surface. Clip gages are then attached between the stationary bridge structure and the ceramic pins to detect pin movement perpendicular to the plane of reference. A schematic of this device is shown in Figure 3. A close-up view of the installed profilometer device is presented in Figure 4.

INSTRUMENT DOMAIN

A systematic way to measure the strain and temperature as a function of distance from the weld centerline needed to be devised. Thus, an instrument domain that incorporated the strain sensors and the thermocouples was designed. A series of strain sensors measuring the strain parallel to the pipe surface were placed both parallel and perpendicular to the fusion line, and thermocouples were welded between the movement markers of each clip gage. These clip gages were spaced along the length of the weld as a function of distance from the fusion line. The profilometer bridge unit was installed across the middle of the instrument domain and all the strain measurement devices for measuring

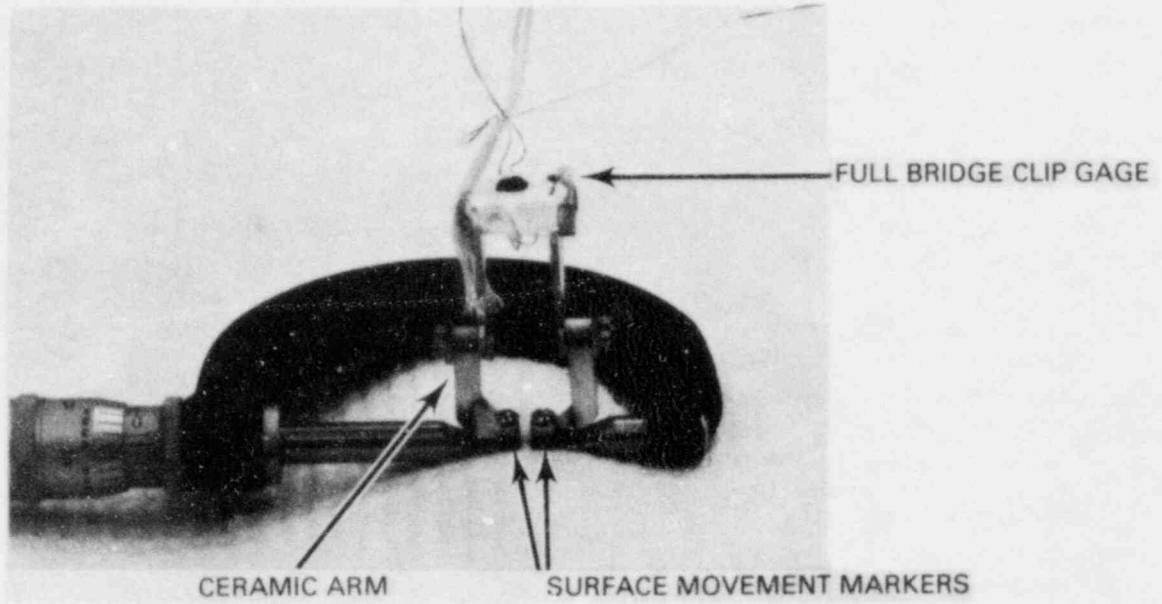


FIGURE 2. Calibration of a Clip Gage

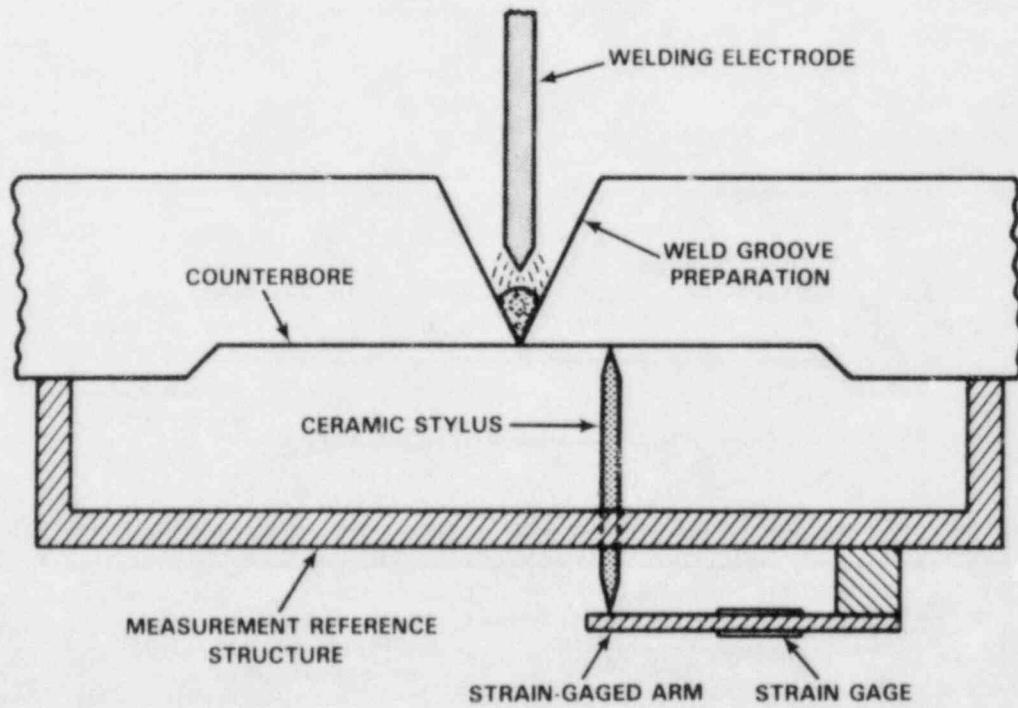


FIGURE 3. Schematic of the Profilometer Used to Measure Strain Perpendicular to the Plate Surface

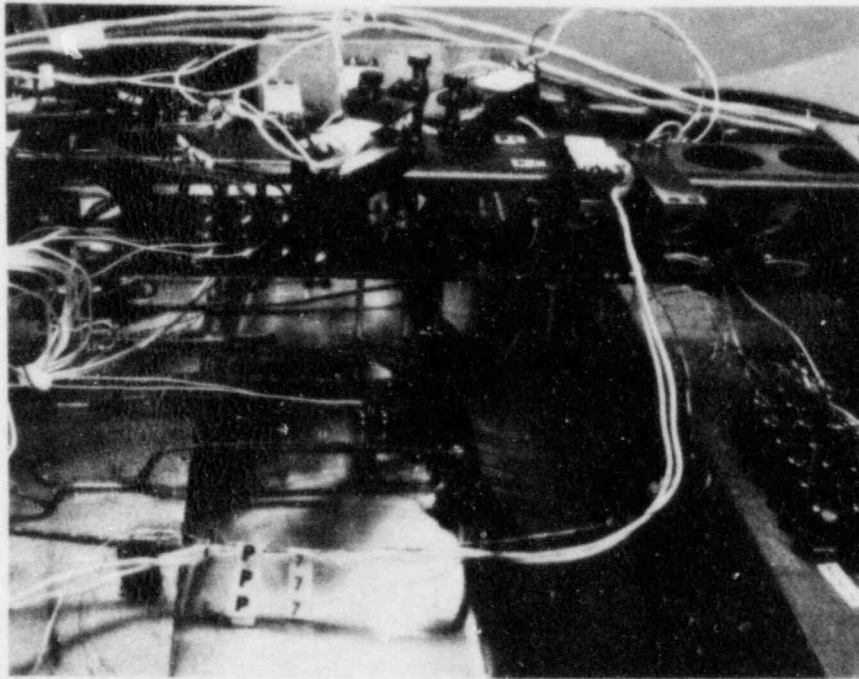


FIGURE 4. Profilometer Unit Attached to a Flat Plate

strain perpendicular to the pipe surface were placed in a straight line perpendicular to the fusion line. A schematic is shown in Figure 5.

An instrument domain was installed on the flat plate feasibility weld to develop installation techniques and for instrumentation checkout. Photographs of this instrument domain are shown in Figures 6 through 8. The surface and thermocouple layout is illustrated in Figure 6 and the profilometer superimposed over the thermocouples and strain sensors in Figures 7 and 8. All of the surface movement markers have been welded in place in Figure 8, but only selected strain measurement devices are in place.

STRAIN MEASUREMENT DEVICE

Several types of clip gages, and two types of insulating legs and movement markers for measuring strain parallel to the surface, have been evaluated. A series of clip gage designs were fabricated at PNL and their effectiveness was compared to commercially available MTS clip gages. The legs of the PNL clip gages were fabricated from titanium and had two different configurations. One configuration was the standard ASTM design that had constant arm widths and therefore exhibited decreasing strain with increasing length along the arm. The second was a constant strain design with sloping arm. Both arm designs were fabricated in varying degrees of rigidity to allow for the wide variation in strain response expected in the HAZ as a function of distance from the fusion line (from microinches to tenths of inches).

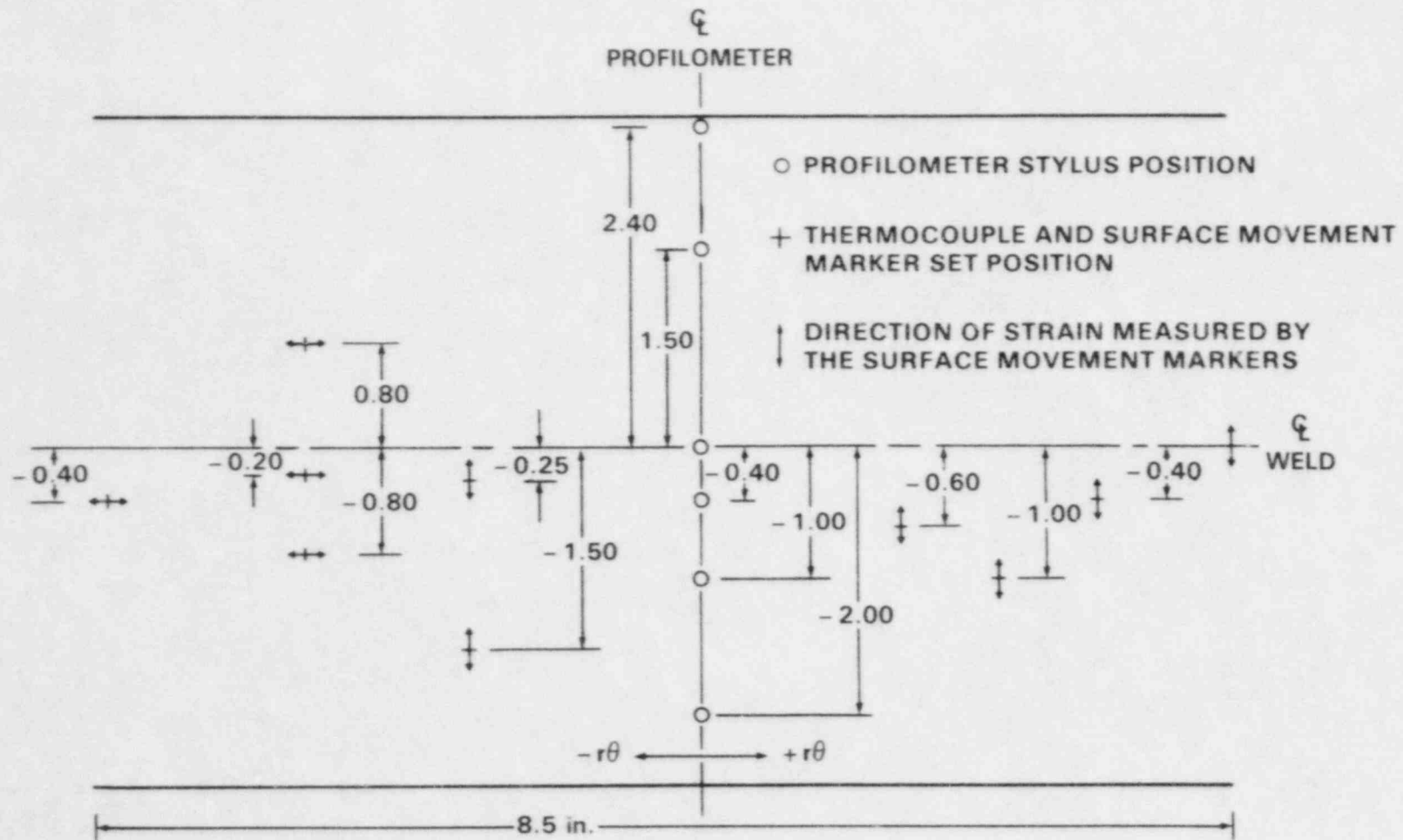


FIGURE 5. Instrument Domain Layout

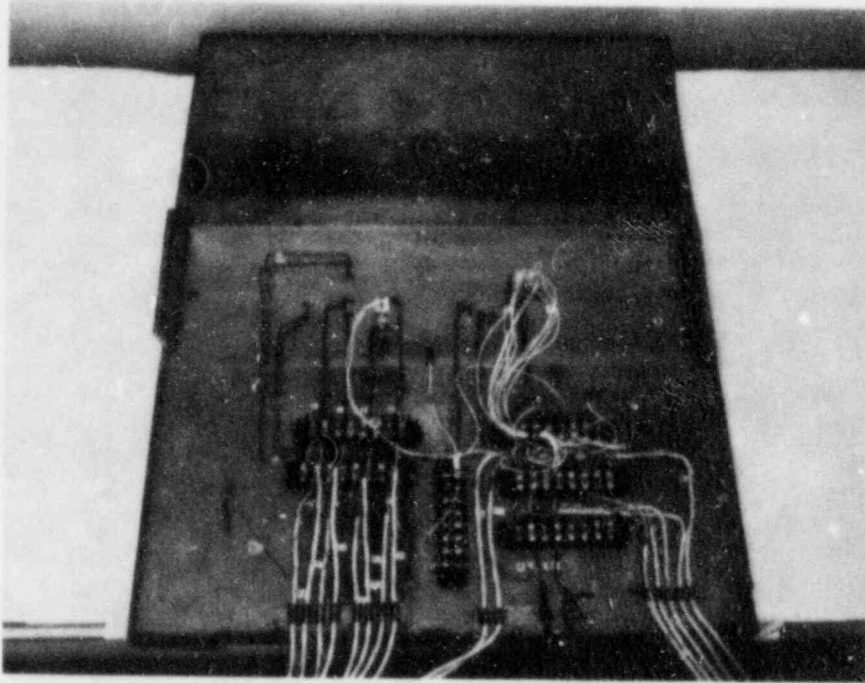


FIGURE 6. Instrument Domain Showing Thermocouple and Surface Movement Marker Layout

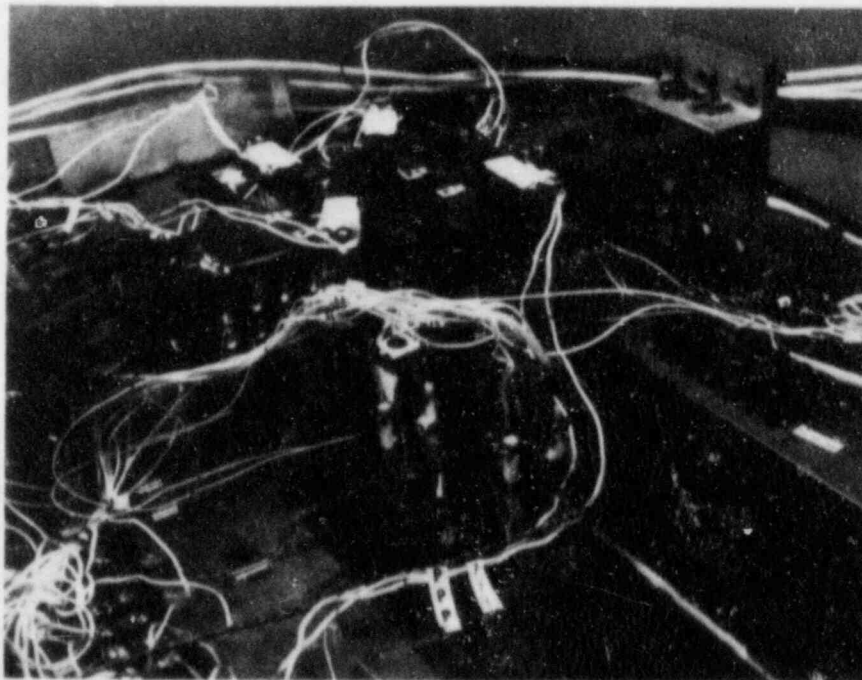


FIGURE 7. Profilometer Unit, Surface Movement Clip Gages, and Thermocouples Attached to the Flat Plate Feasibility Weld

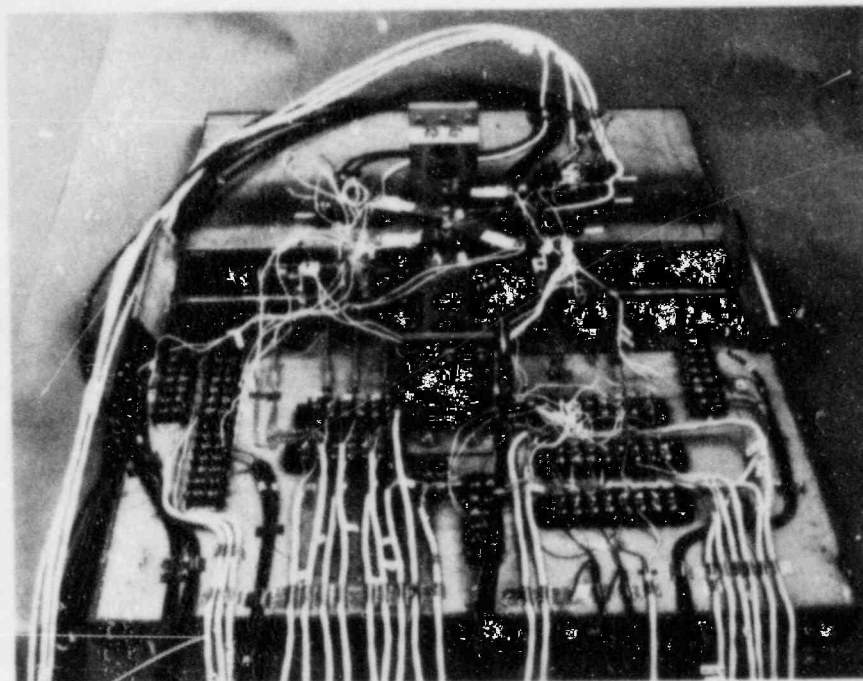


FIGURE 8. Instrument Domain Showing Profilometer Superimposed over Thermocouple and Surface Movement Marker Layout

A constant-strain clip gage was instrumented with a series of thermocouples along the length of the arm to determine the maximum temperature of the strain gage on the metallic portion of the clip gage. It was desirable to keep the temperature of the strain gage below 250°F (~120°C). The thermocoupled clip gage was then moved to various positions in the instrument domain. A no-filler-metal root pass was made for each of these domain positions to determine whether the ceramic arms were efficient enough to make the gage useful at all positions. It was found that the temperature remained below 250°F for all positions tested.

A full bridge strain gage was attached to the ceramic arms and calibrated for mV per unit strain using a blade micrometer, as shown in Figure 4. The initial PNL gage was tested before final cure and found to be relatively stable, with a strain measurement reading of ~10 μ in. of travel per mV output. Several more of these gages were fabricated and all of them were given a final stabilization treatment and protective coating. The gages were then rechecked and were found to be less stable than they were before the final stabilization treatment. The reason for this decrease in stability is presently being investigated.

Commercially available clip gages were ordered from MTS and adapted for use with ceramic arms. This required a different ceramic arm and surface movement marker design from those used with the PNL gages. The resultant strain

sensing device is shown in Figure 9. These devices show high stability and good strain measurement capability with typical resolutions of 10 μ in. of travel per mV output.

FLAT PLATE FEASIBILITY WELD

The instrumentation package was tested using a flat plate feasibility weld. A 1-in. thick, Type 304 SS plate was selected for this weld. Its thickness corresponds to that of the 24-in.-dia Schedule 80 Type 304 SS pipe that will be used in the initial TM determination experiments. A "V" groove weld preparation was machined into the plate, and a 2T counterbore region was prepared for installation of the instrument domain.

A complete instrument domain was placed on the plate, including surface markers, thermocouples and the profilometer support structure. The completed domain with several clip gages attached is shown in Figure 8.

The initial instrument tests on this plate were run using a wash-pass technique. The plates were first joined with an autogenous root pass (Pass 1) with a heat input of 16 kJ/in. Seven no-filler-metal wash root passes (Passes 2 through 8) were made at the same heat input as the original root pass. Two filler-metal passes (Passes 9 and 10) were then made at a heat input of 35 kJ/in.

Various instrumentation configurations were used during these feasibility passes. Passes 1 through 3 were run with only the thermocouples and a thermocoupled non-strain-gaged clip gage, to determine whether the ceramic arms provided sufficient thermal insulation to protect the strain gages that would be

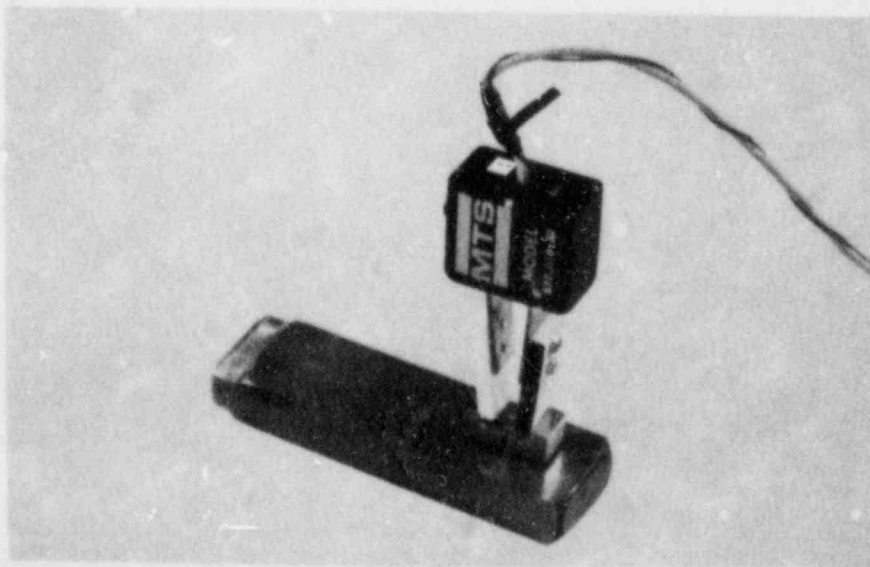


FIGURE 9. MTS Strain Sensing Units Adapted for High-Temperature Use

installed on the clip gage arms. Passes 4 through 8 were run with the thermocouples and one experimental clip gage. The clip gage was moved to various surface marker positions during a series of wash passes, to establish whether the gage had sufficient sensitivity to be usable at many positions, and to determine the order of magnitude of the strain induced at the various positions.

The data for the first eight passes were recorded with a Fluke Data Logger, as the DRAS was still under construction. The data logger operated at a rate of one data set every 10 s. Selected temperature histories, collected during Pass 8, are plotted as a function of distance from the fusion line in Figure 10. The plot depicts the change in temperature at various distances from the fusion line. The curves show a sharp temperature rise as the arc approaches and a relatively slow cool-down after the arc has passed. The heating rate and the maximum temperature decrease as the distance from the fusion line increases. The temperature profiles show that the arc induces a temperature rise more than 1.5 in. from the fusion line.

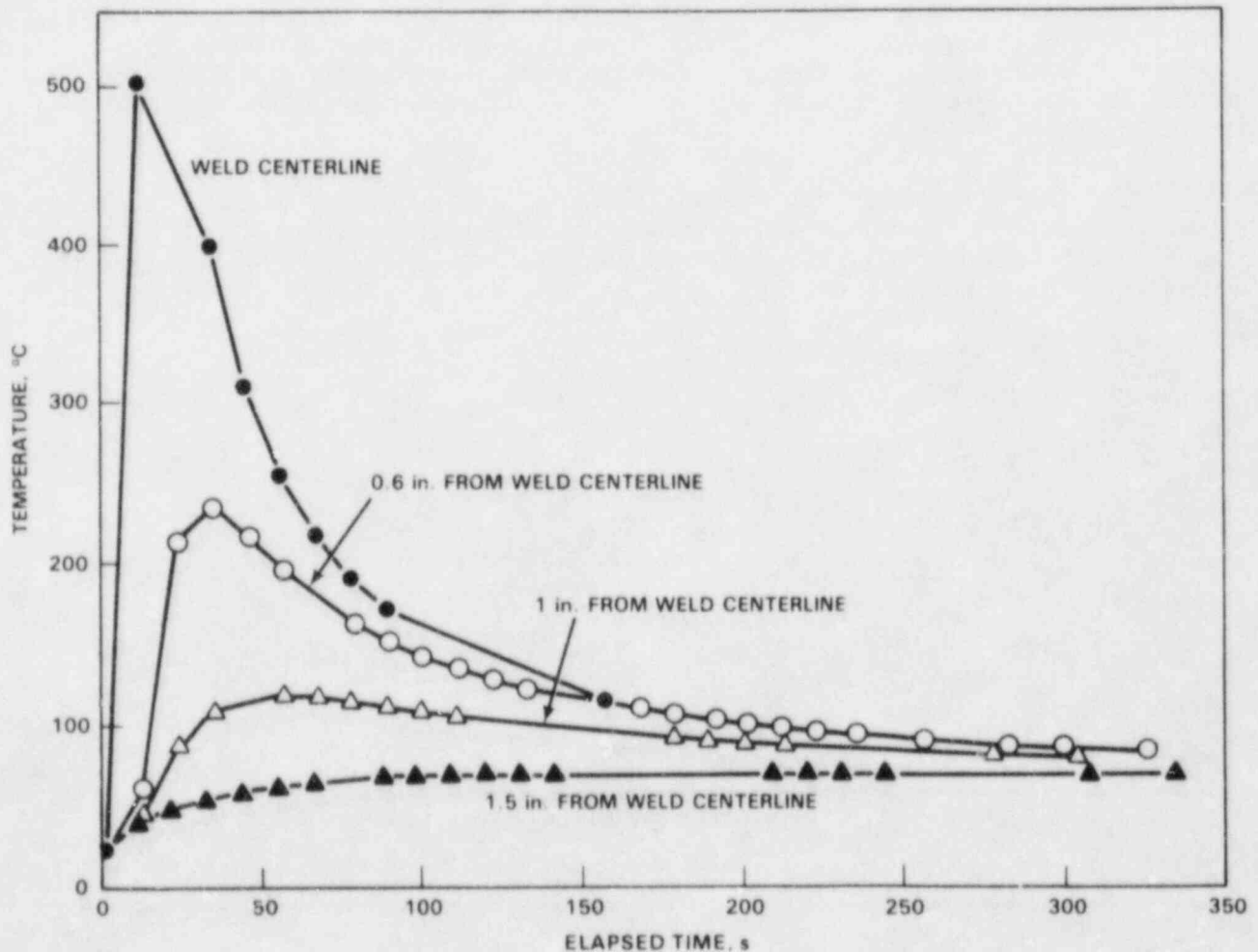


FIGURE 10. HAZ Surface Profiles After Initial Temperature Rise

A composite view of the traveling temperature profile on the plate surface can be developed from the multiple temperature/time plots by determining the time when the arc is perpendicular to the temperature indicator and then superimposing the plots, using the time when the arc was perpendicular to the temperature sensor as a normalization basis. A composite view of the temperature profile in the surface of the plate surrounding the arc is shown in Figure 11. The profile exhibits a sharp temperature gradient as well as an increasing lag time before the maximum temperature after arc passage is reached as distance from the fusion line increases.

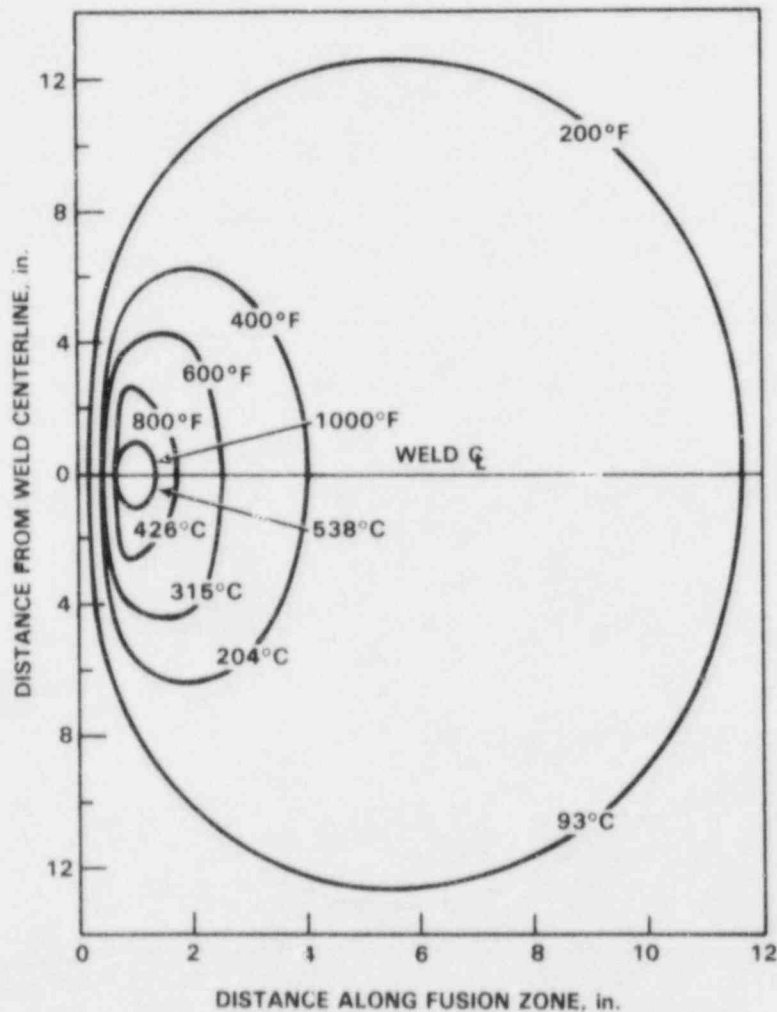


FIGURE 11. Two-Dimensional Surface Thermal Profile Around Arc

The tenth pass was the second filler-metal pass and was run under the same welding conditions as Pass 9. Five clip gages were placed on surface markers and four clip gages were connected to the profilometer. The data for this weld were passed through the Fluke Data Logger and collected for analysis on an Apple computer at a rate of 8 s per complete data set. Data storage problems were encountered during the later segment of the weld pass and the data for the last portion of the weld were lost; therefore, the data time span for Pass 9 is misleadingly short.

Maximum temperature as a function of distance from the fusion line was comparable for all ten passes, as shown in Figure 12. The temperature rise, however, was so rapid that the peak temperature was missed by a data collection rate of one data set every 8 to 10 s. Therefore, an independent thermocouple was attached at the weld centerline during Pass 10, and a high-speed recorder monitored the temperature rise and recorded the exact maximum temperature. The maximum temperature discrepancy for Pass 10 is illustrated by the comparison of the data-logger-collected data with the strip-chart-recorded data for weld centerline thermocouples in Figure 12. The maximum temperature determined by the Fluke Data Logger data gathering system was several hundred degrees below that recorded with the strip chart recorder. This problem will be eliminated once the DRAS is operational.

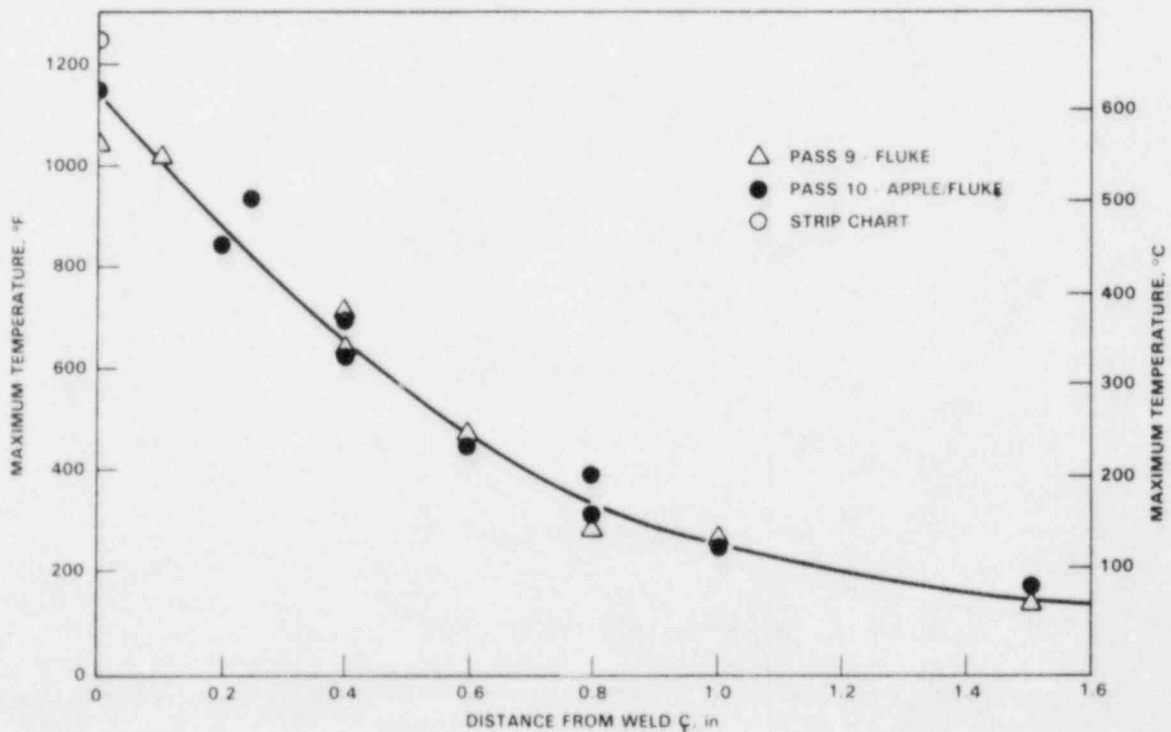


FIGURE 12. Flat Plate Weld Surface Temperature Gradient

The strain measurements (in mV) from the surface clip gages are compared with their respective temperature profiles in Figures 13 through 17. A compressive wave was initially observed, changing to a tension mode once a temperature increase began. Note that the time required for the temperature and strain to reach their maximum values is essentially the same. The time when the arc is perpendicular to the temperature sensor is indicated on the time/temperature and time/strain plots. The time at initial temperature rise is indicated on the time/strain plot.

Figure 18 presents all of the time/strain plots grouped as a function of strain direction. One set contains the strains measured perpendicular to the fusion line while the other set contains those measured parallel to the fusion line. It appears that the maximum tensile strain is reached before the arc becomes perpendicular to the sensor for the strains measured perpendicular to the fusion line, but after the arc becomes perpendicular for the strains parallel to the fusion line. If so, this phenomenon may be related to the difference in restraint between plate material parallel to and perpendicular to the welding direction.

A comparison of the absolute magnitude of the three gages oriented parallel to the welding direction is shown in Figure 19, and of the two clip gages oriented perpendicular to the welding direction in Figure 20. The magnitude of strain decreases with increasing distance from the weld centerline; and the magnitude of strain parallel to the welding direction is considerably greater than that perpendicular to the welding direction.

The type of data generated by the profilometer during welding is illustrated in Figure 21. The constantly changing portion of the strain readout indicates that the plates are contracting due to shrinkage stresses during the complete weld pass. The axis of bending is the centerline of the weld and the bending tends to close the weld groove. The plot also indicates that a thermally-induced deformation bump travels with the weld pool independently of the plate-bending phenomenon.

A composite of the various profilometer gage outputs, Figure 22 shows that the time the maximum height of the bump is reached lags farther and farther behind that for the weld centerline time as the perpendicular distance from the fusion line increases. The bump first appears ~2 in. in front of the arc and is still evident more than 10 in. behind it. These results are based on the travel speed of the arc and the time during which the deformation readings are above the "constant" rate of bending deformation before and after the bump passes. The maximum height cross section of the bump is plotted in Figure 23 and indicates that the width of the bump is at least 3 in. and that the maximum height is over 0.010 in. A two-dimensional plot of the thermal bump profile, based on the time when the arc is perpendicular to the origin, is depicted in Figure 24.

A composite plot of the surface strains in all three directions and their relationship to the time/temperature plot is shown in Figure 25. It is anticipated that analysis of this type of strain/temperature/time data will yield full characterization of the TM history of the pipe welds fabricated in the program.

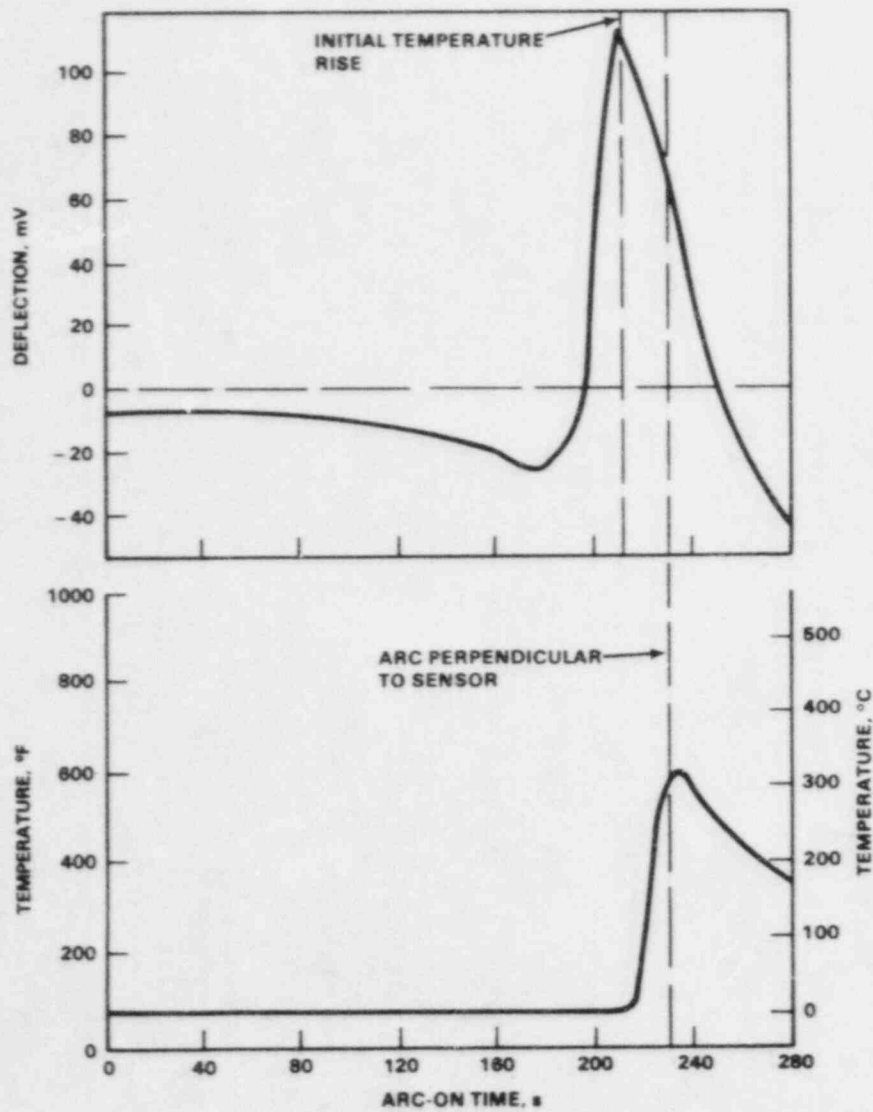


FIGURE 13. Surface Strain Parallel to Welding Direction, and Temperature 0.2 in. from Weld Centerline

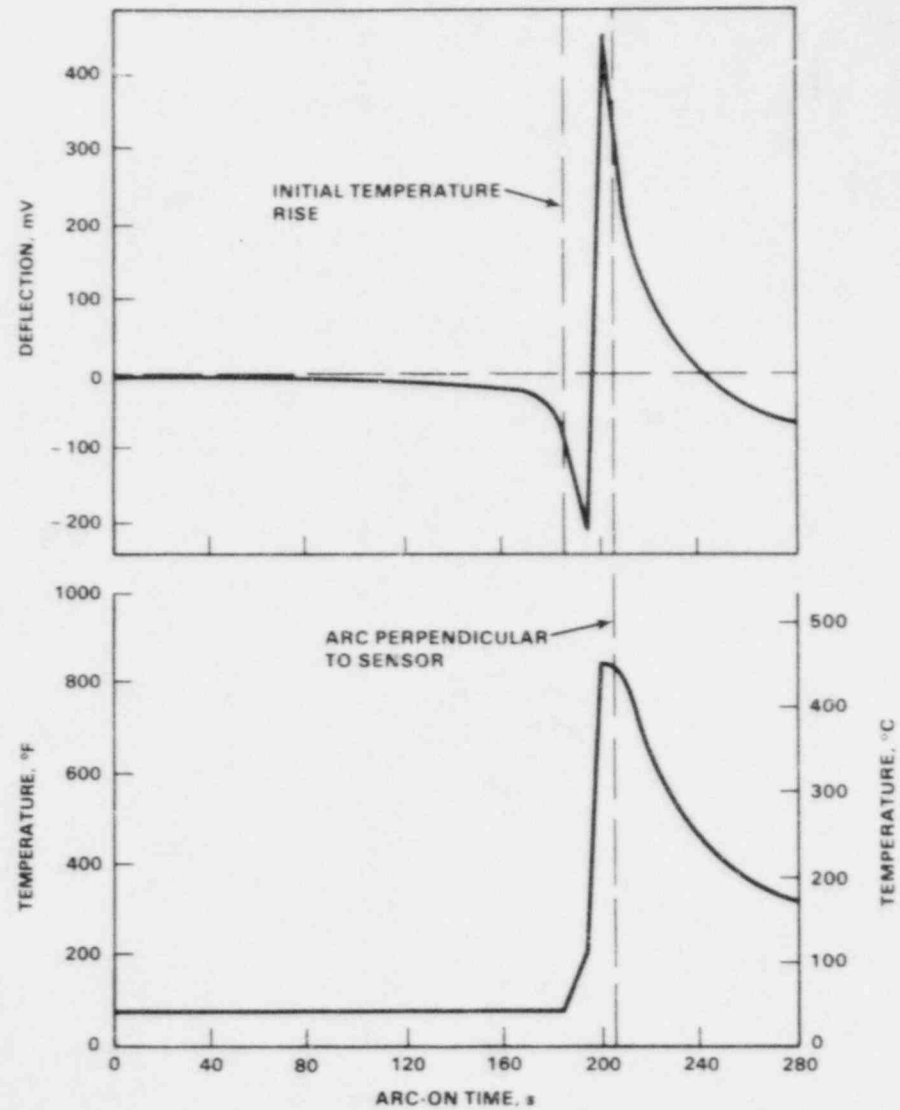


FIGURE 14. Surface Strain Parallel to Welding Direction, and Temperature 0.4 in. from Weld Centerline

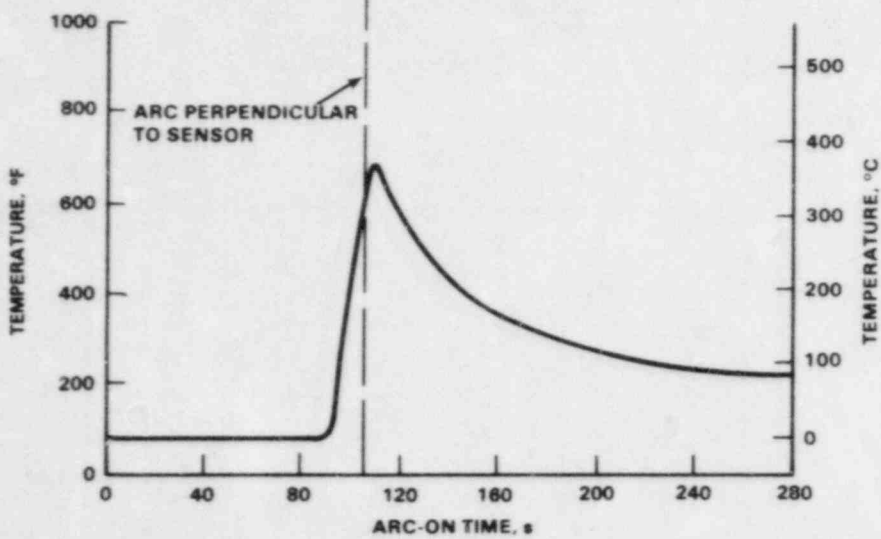
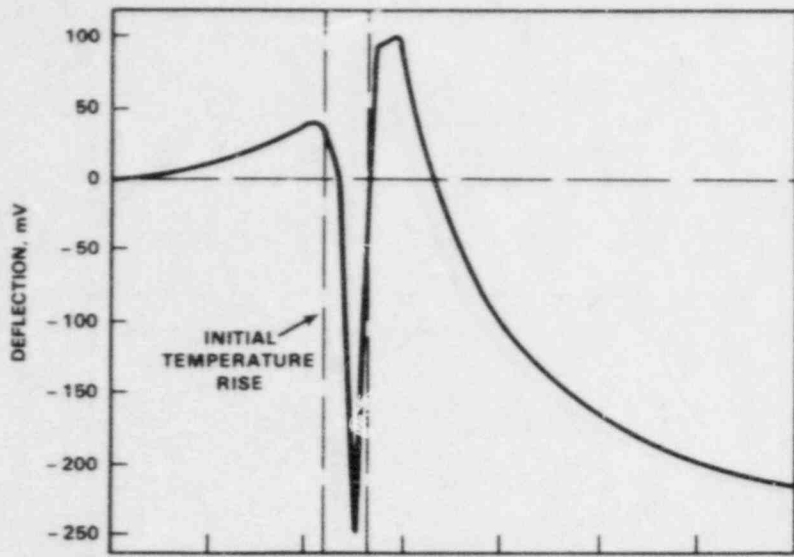


FIGURE 15. Surface Strain Perpendicular to Welding Direction, and Temperature 0.4 in. from Weld Centerline

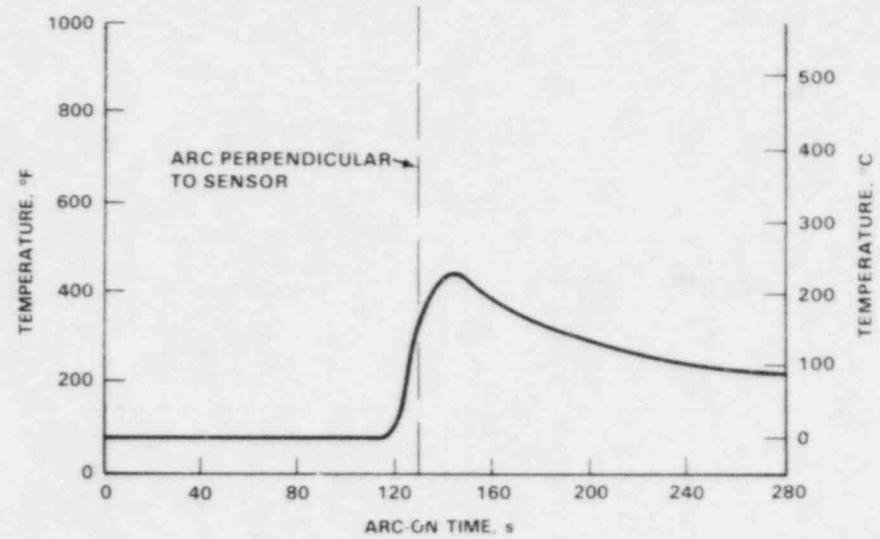
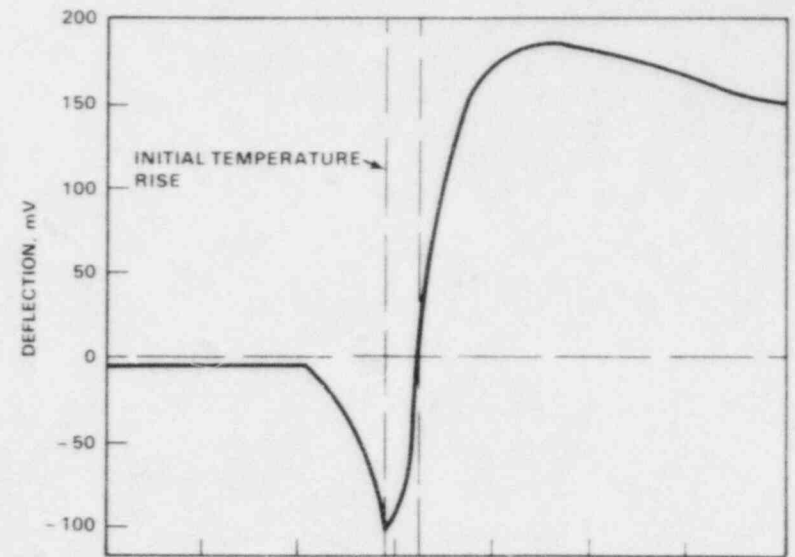


FIGURE 16. Surface Strain Perpendicular to Welding Direction, and Temperature 0.6 in. from Weld Centerline

17

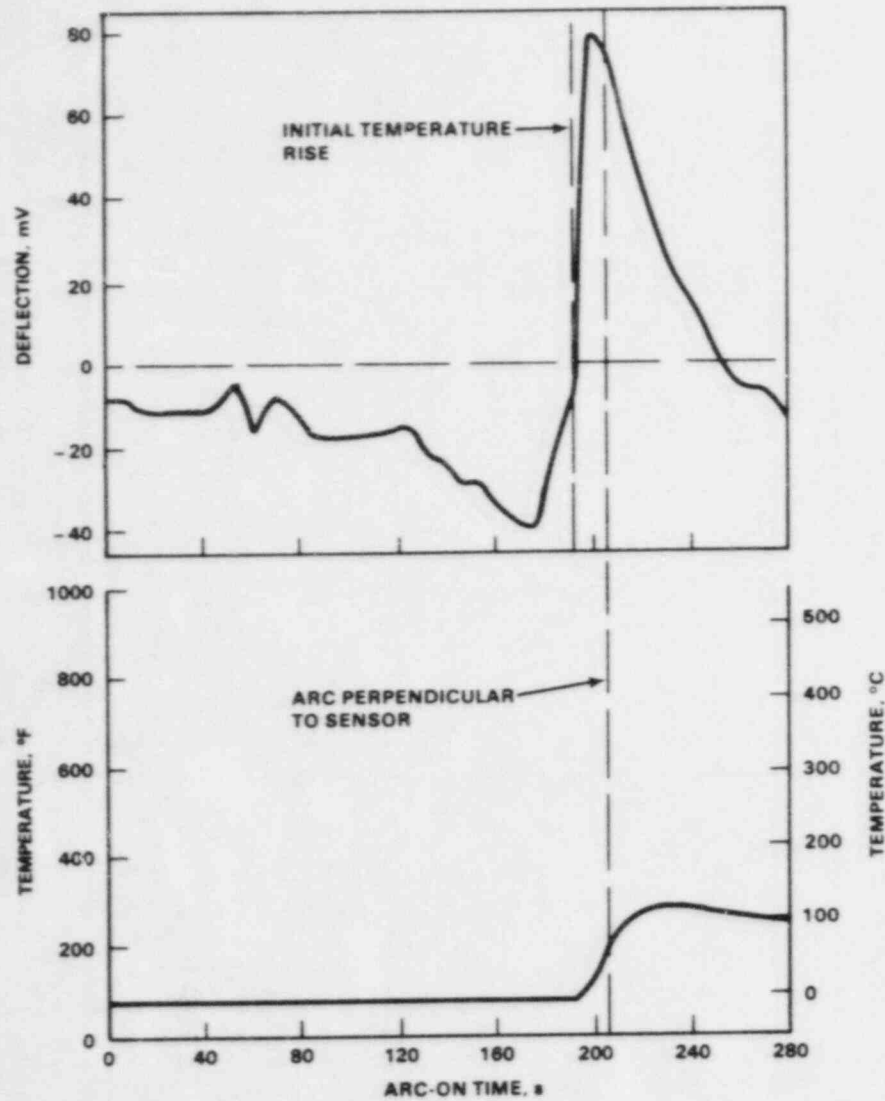


FIGURE 17. Surface Strain Parallel to Welding Direction, and Temperature 0.8 in. from Weld Centerline

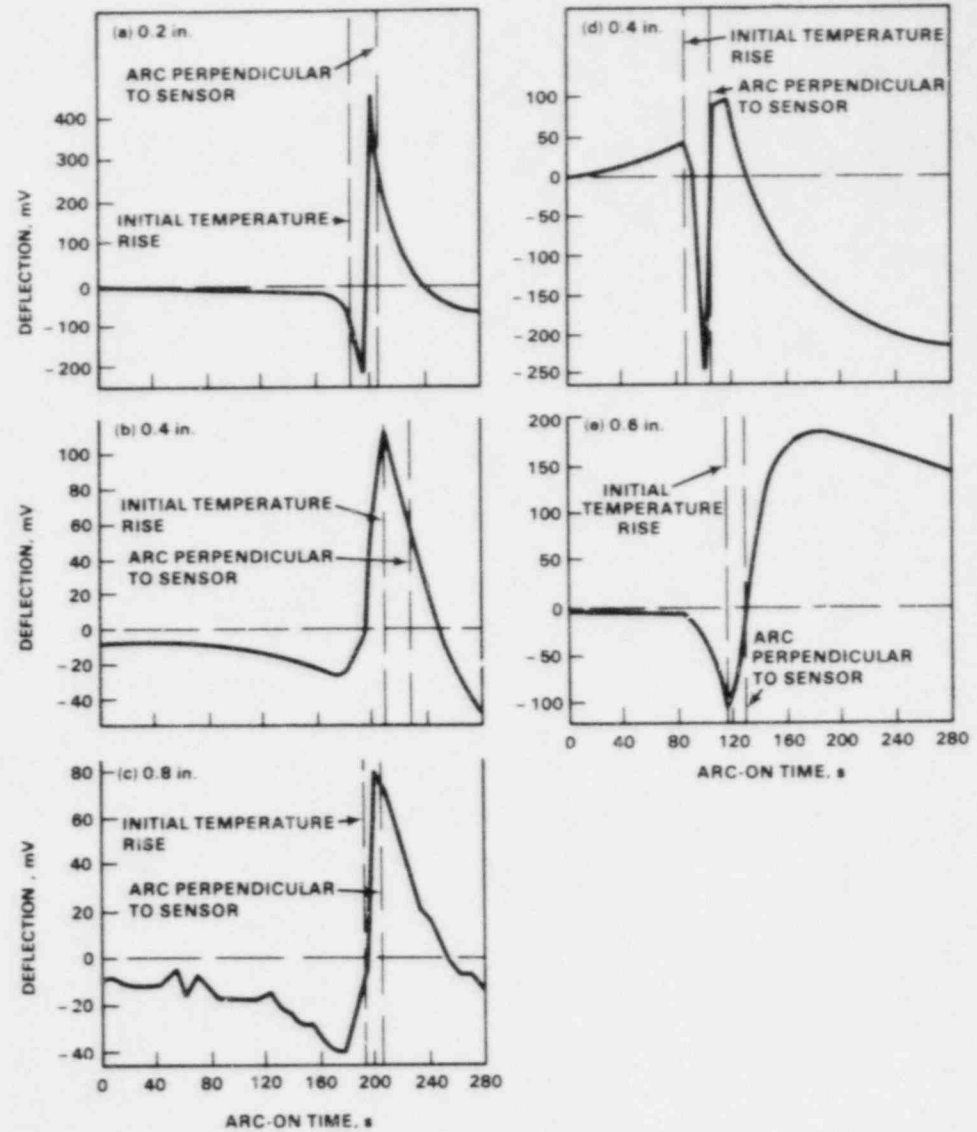


FIGURE 18. Comparison of Strain Changes During Welding as a Function of Distance from the Fusion Line and Direction of Strain. (a) through (c): strain parallel to welding direction; (d), (e): strain perpendicular to welding direction.

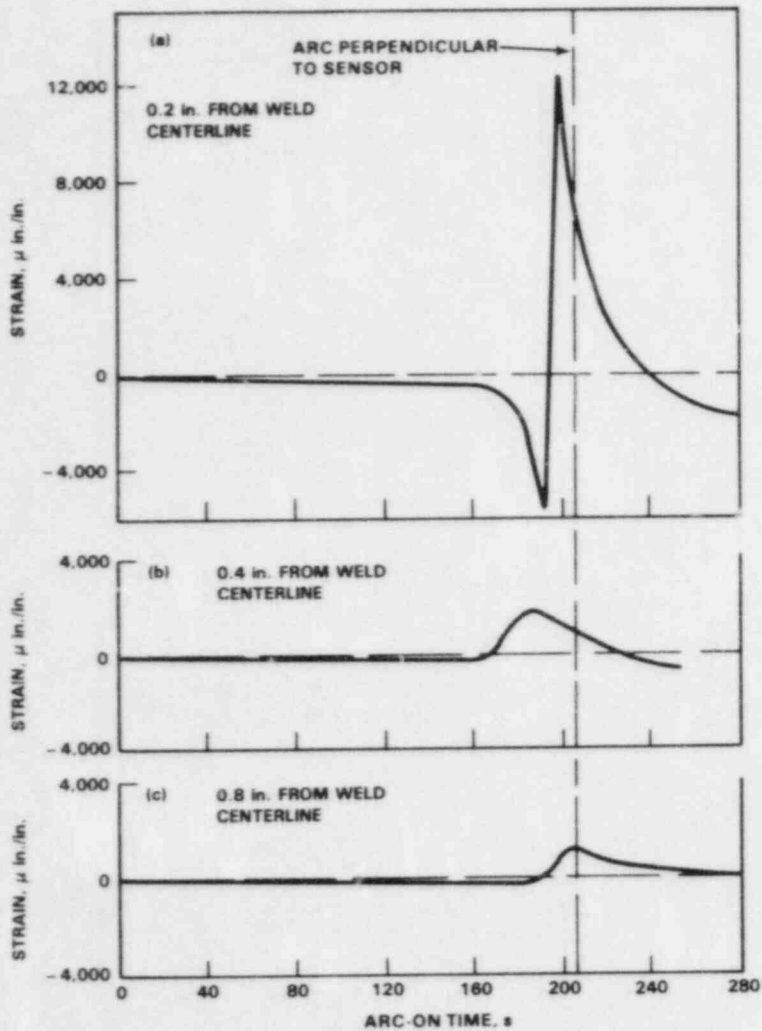


FIGURE 19. Strain Measurements from Gages Parallel to Welding Direction

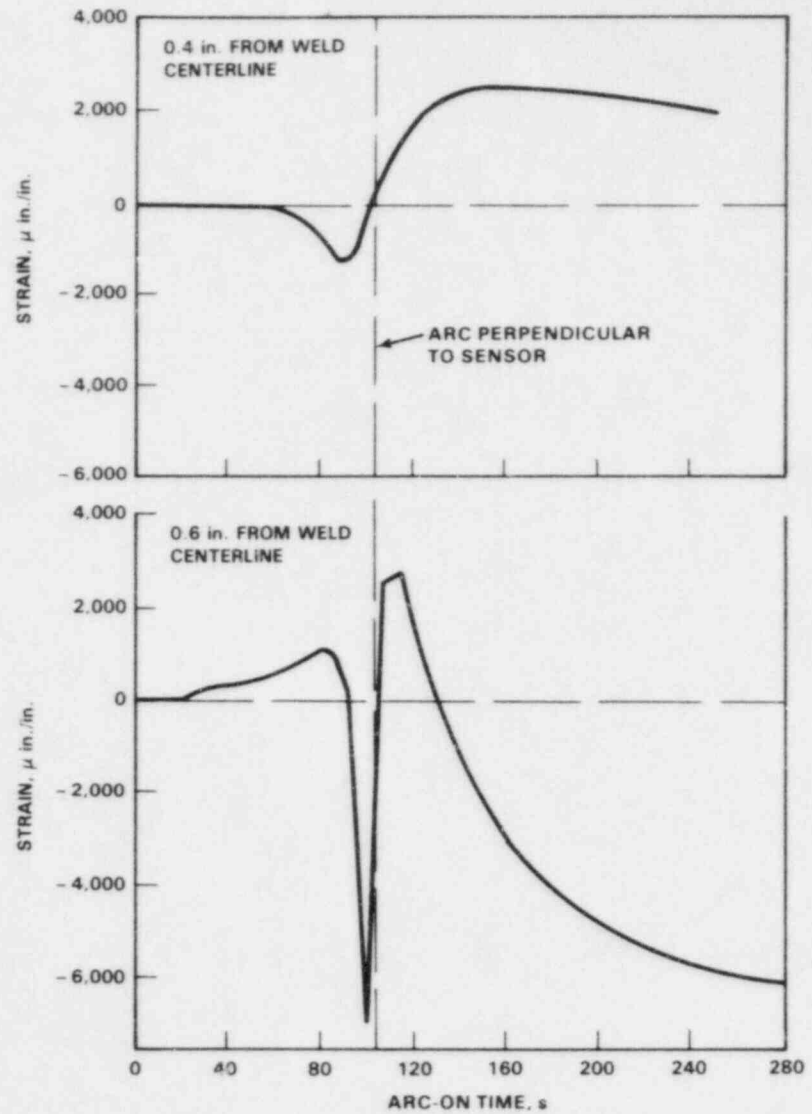


FIGURE 20. Strain Measurements from Gages Perpendicular to Welding Direction

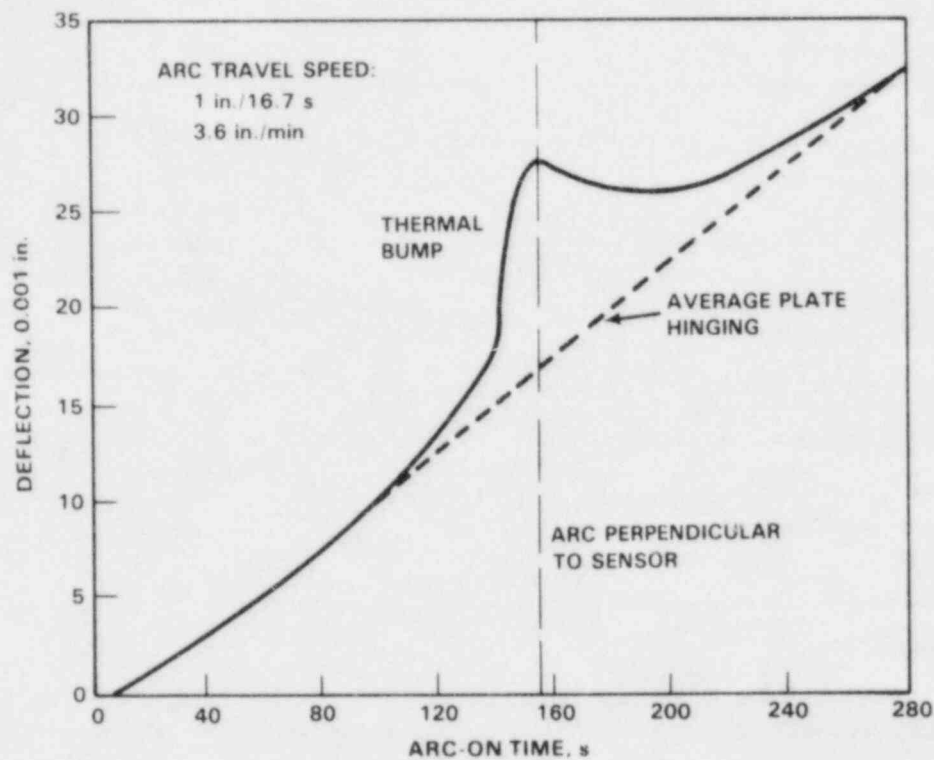


FIGURE 21. Surface Movement Perpendicular to Plate Surface at Weld Centerline

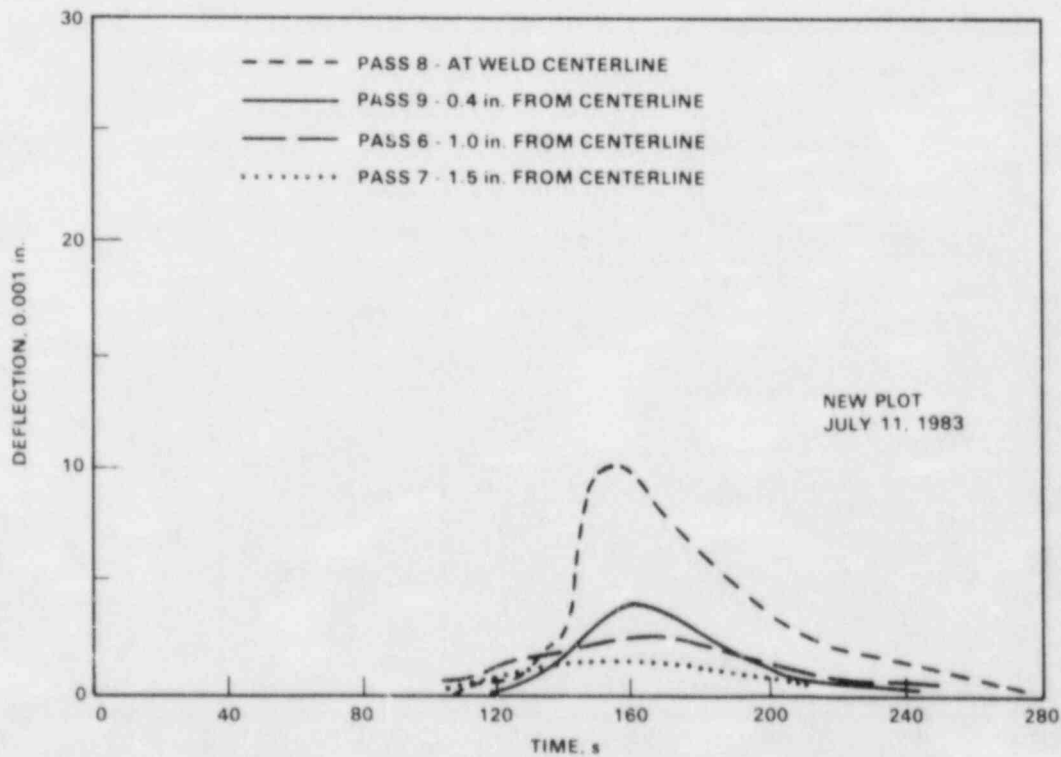


FIGURE 22. Thermal Bump Displacement as a Function of Distance from the Weld Centerline

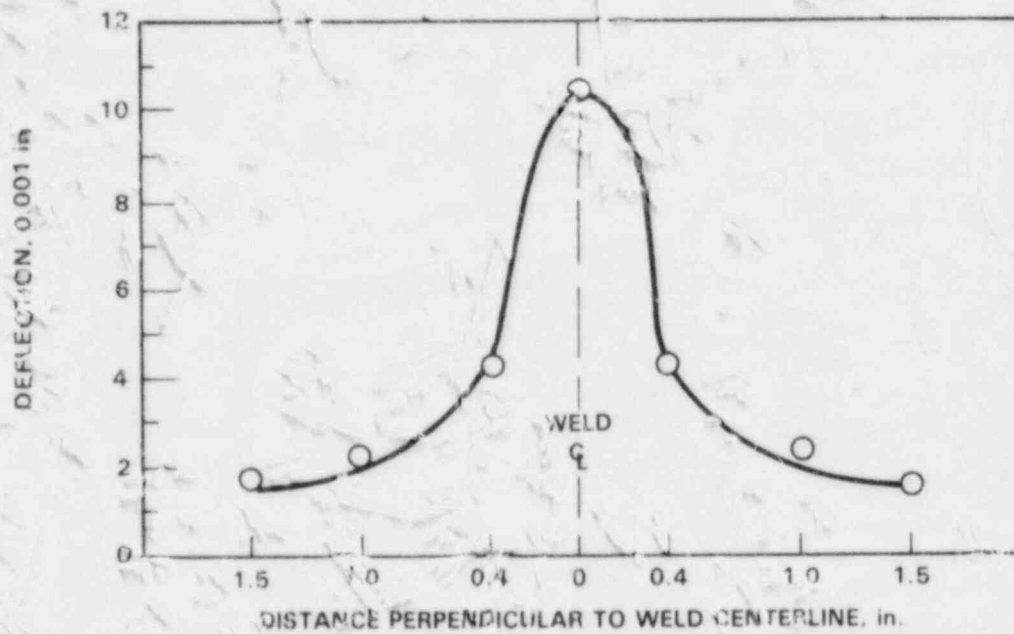


FIGURE 23. Thermal Bump Height as a Function of Distance from the Weld Centerline

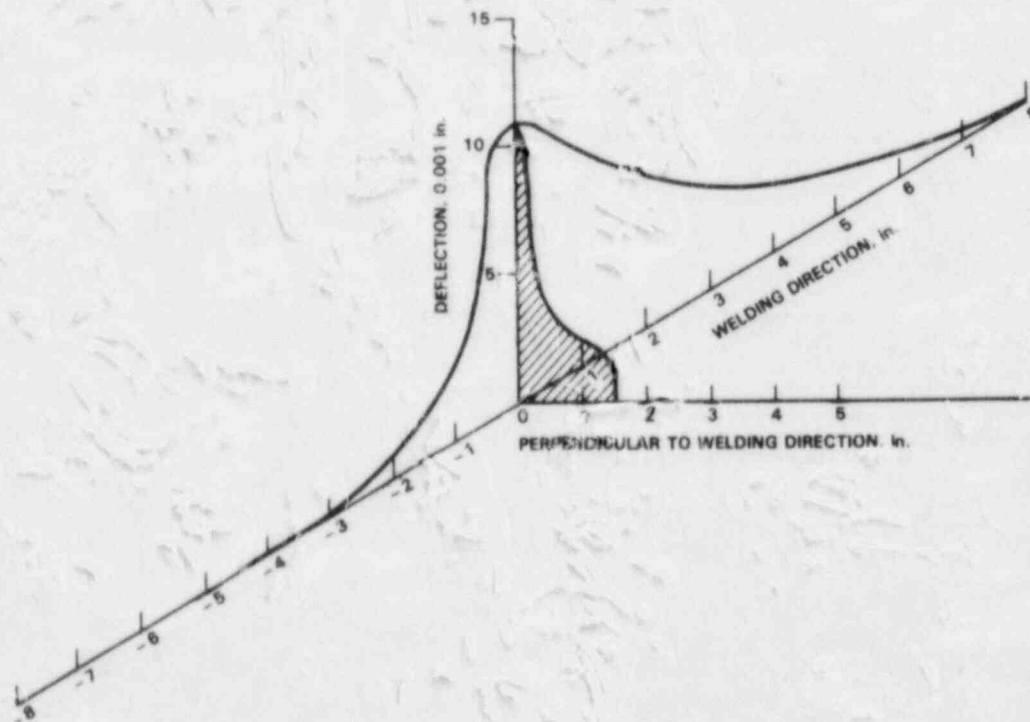


FIGURE 24. Three-Dimensional Representation of the Thermal Bump Induced at the Plate Surface During Welding

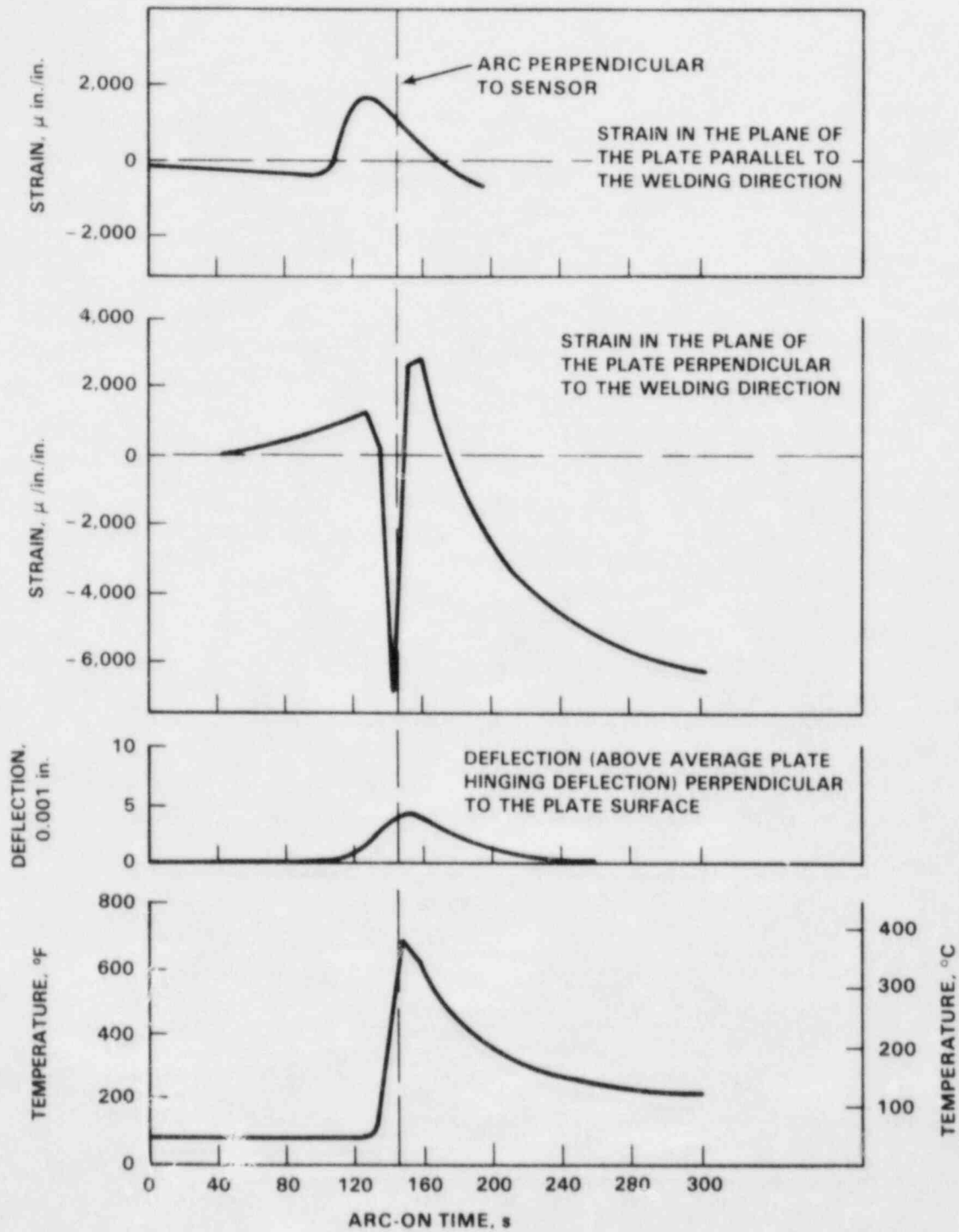


FIGURE 25. Surface Movement 0.4 in. from the Fusion Line in the x, y, and z Directions Correlated with the Weld-Induced Change in Temperature

INTERACTIONS WITH OTHER LABORATORIES

R. C. Page and D. G. Atteridge visited E. Merrick at Tennessee Valley Authority (TVA) and C. D. Lundin at the University of Tennessee (UT) to discuss potential program interactions. TVA agreed to provide surplus Type 304 and 304L primary piping. If deemed necessary, UT agreed to provide "field welding" of these pipes and weld simulation specimens derived from the TM histories measured on the pipe welds that UT would make.

W. E. Wood, Oregon Graduate Center (OGC), agreed to produce weld simulation specimens from TM histories supplied by PNL. He and his staff modified an existing Apple-based TM history recording system into a field welding TM monitor. The system is capable of collecting 64 channels of data at a rate of less than one cycle per second for the 64 channels. It is proposed that the system be used on instrumented field weldments fabricated at PNL, OGC, and/or TVA.

TASK II. INFLUENCE OF COMPOSITION AND THERMOMECHANICAL HISTORY ON DOS AND IGSCC

Austenitic SS may become sensitized and thus susceptible to IGSCC when chromium-rich carbides precipitate at grain interfaces, causing a chromium depletion of the adjacent matrix. This phenomenon is controlled by the thermodynamics of carbide formation and the kinetics of chromium diffusion. In a temperature regime where chromium carbide precipitation is thermodynamically stable (<800°C) and chromium diffusion is sufficiently rapid (>500°C), a SS can become sensitized in a relatively short time.

Stress corrosion cracking of SS has been studied extensively for more than 20 years. However, much of the data that has been generated cannot be directly applied to the understanding and prediction of weld-induced sensitization. The development of a sensitized microstructure depends on a material's bulk composition and TM history. Neither of these factors, nor their effect on IGSCC, is sufficiently understood for accurate predictive modeling.

The primary objective of this task, therefore, is to develop a sufficient data base to predict DOS and IGSCC susceptibility as a function of TM history and material composition. Experimentation will involve weld simulation and small-diameter pipe weld parametric studies. Selected isothermal testing will also be conducted to gain a quantitative understanding of thermal and compositional effects on DOS. All data will be used in developing a DOS prediction methodology based on thermodynamic and kinetic models. An empirical correlation between DOS and IGSCC susceptibility will be determined in specific reactor-relevant environments, providing a basis for IGSCC susceptibility prediction methodology.

DEGREE OF SENSITIZATION MEASUREMENT

A significant limitation of much of the DOS measurements in the literature is the lack of technique sensitivity and quantification for a range of DOS values. The electrochemical potentiokinetic reactivation (EPR) test, however, has these features and will be used to evaluate bulk composition and TM history effects on DOS. Capability development at PNL will be demonstrated in tests on DOS standards using both laboratory and field cell techniques.

PNL has set up two methods for DOS measurement by EPR: a semi-automatic system, InstruSpec Model WC-5, and a potentiostat/galvanostat system, PAR Model 173 with a PAR Model 175 universal programmer. All of the reported data were collected with the Model WC-5 system and a test solution of 0.5 M H₂SO₄ + 0.01 M KSCN, unless otherwise noted.

PNL contributed to the EPR round robin testing that was organized by ASTM Committee G1.08. Test specimens were obtained from W. L. Clarke of General Electric (GE)-Vallecitos. The results were in good agreement with those produced by similar tests at GE and Argonne National Laboratory (ANL), and were well within the standard deviation of the first series of ASTM round robin

tests (in which eight laboratories participated). The largest data discrepancy among individual investigators was in the normalization from grain size determinations.

A more complete set of internal PNL EPR standards for Type 304 SS will be selected from the carbon series specimen test matrix. Over fifty Type 304 SS specimens have been heat-treated at PNL to produce a range of EPR values from 0 to more than 100 coulombs per square centimeter (C/cm^2). Particular emphasis will be placed on specimens (of various bulk compositions) with EPR values from 0.1 to 10 C/cm^2 . These selected specimens will undergo testing at several laboratories to assess measurement consistency, and will be used as test standards throughout the program to ensure operator competency.

Measured EPR values (i.e., charge density normalized by grain boundary area) depend on a number of test and material parameters, which must be kept constant to obtain quantitative DOS measurements. The importance of some of these parameters was demonstrated during the ASTM standards testing. Moderately to severely sensitized Type 304 SS was observed to be very responsive to minor changes in solution temperature. An example of this behavior is shown in Figure 26. The EPR value increased ~ 2 to 4 C/cm^2 per $^\circ C$, depending on material DOS. This indicates that quantitative and reproducible laboratory results may necessitate better temperature control than the $\pm 2^\circ C$ suggested by Clark.¹ A temperature control of $\pm 0.5^\circ C$ has been maintained for all EPR tests at PNL.

Surface preparation of EPR test specimens is known to be a critical step in obtaining reproducible DOS measurements, particularly for field applications. Two alternative methods of field application/surface preparation for EPR analysis are being investigated: 1) pre-polarization in the active dissolution range, and 2) electropolishing. Pre-polarization, or activation, of the

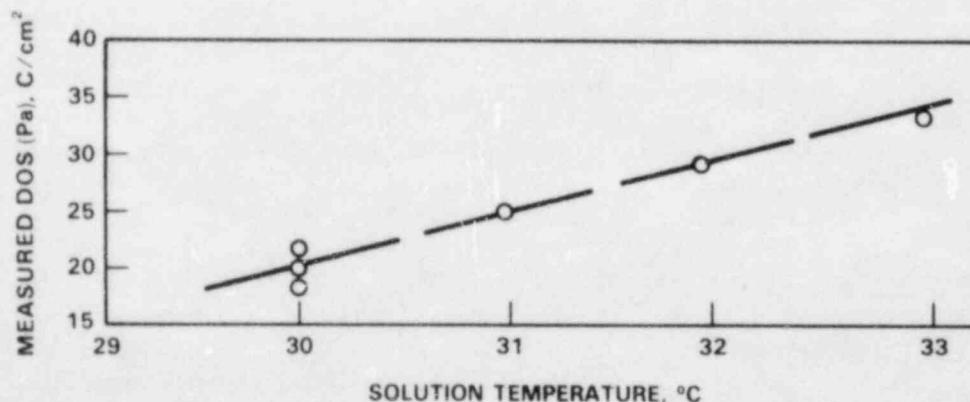


FIGURE 26. EPR Measurements on a Severely Sensitized Type 304 SS Specimen as a Function of Test Solution Temperature

specimen surface was evaluated using four furnace-sensitized Type 304 SS materials with different DOS levels. Each specimen was mechanically polished to a 600-grit finish and activated at a potential of -0.2 V (SCE). The effect of time at this potential on the resultant EPR-measured DOS for several alloys (see Table 1) is shown in Figure 27. Measurements on 1- μ m diamond-polished surfaces are plotted on the y axis for comparison. Preliminary results indicate that activation times of 30 to 60 s are the most consistent for standard diamond-polished specimens. Surface preparation differences between standard and activated analysis techniques are illustrated in Figure 28. The activated surfaces exhibit considerably more polishing-induced surface grooving than the standard surface processing technique, but the pitting distribution appears to be relatively unaffected by this difference. Tests are continuing in an attempt to calibrate this technique for use in documenting weld HAZ sensitization.

Scoping tests were also initiated to evaluate electropolishing techniques for surface preparation. Various phosphoric-glycerin solutions and 70 wt% phosphoric acid were selected for tests on a severely sensitized Type 304 SS under designated potential/current conditions. Surface appearance will be examined after electropolishing and EPR testing. These EPR results will be compared to those from specimens with a 1- μ m diamond-polished surface.

An important aspect of this subtask is HAZ DOS evaluation. A miniaturized cell and reference electrode (InstruSpec Model 750) was purchased for field DOS measurements. Quantification tests comparing the field and laboratory cells were conducted at room temperature and at 30°C. Results summarized in Table 2 are for activated analysis tests on specimens mechanically polished to a 600-grit finish. As the table shows, the largest difference between the two systems resulted from the use of the miniature reference electrode (MRE). Field cell EPR tests results were identical to laboratory cell results when the MRE was used in both cells. The MRE produced consistently higher corrosion potentials (E_{corr}) and lower breakaway potentials (E_B) than a standard reference electrode. However, the final EPR charge density values were in most cases within the normal data scatter.

TABLE 1. Composition of Carbon Series Alloys (Type 304 SS), wt%

Alloy	C	Cr	Ni	Mn	Si	Mo	N	S	P
C1	0.015	18.6	9.0	1.8	0.45	0.13	0.08	0.003	0.019
C2	0.020	18.4	9.0	1.7	0.50	0.23	0.10	0.009	0.033
C3	0.035	18.2	8.7	1.7	0.60	0.28	0.07	0.009	0.022
C4	0.045	18.2	8.4	1.7	0.75	0.19	0.09	0.005	0.022
C5	0.050	18.5	8.9	1.8	0.60	0.16	0.10	0.007	0.021
C6	0.062	18.4	8.7	1.8	0.40	0.20	0.07	0.013	0.015
C7	0.072	18.5	9.3	1.7	0.46	0.43	0.04	0.017	0.046

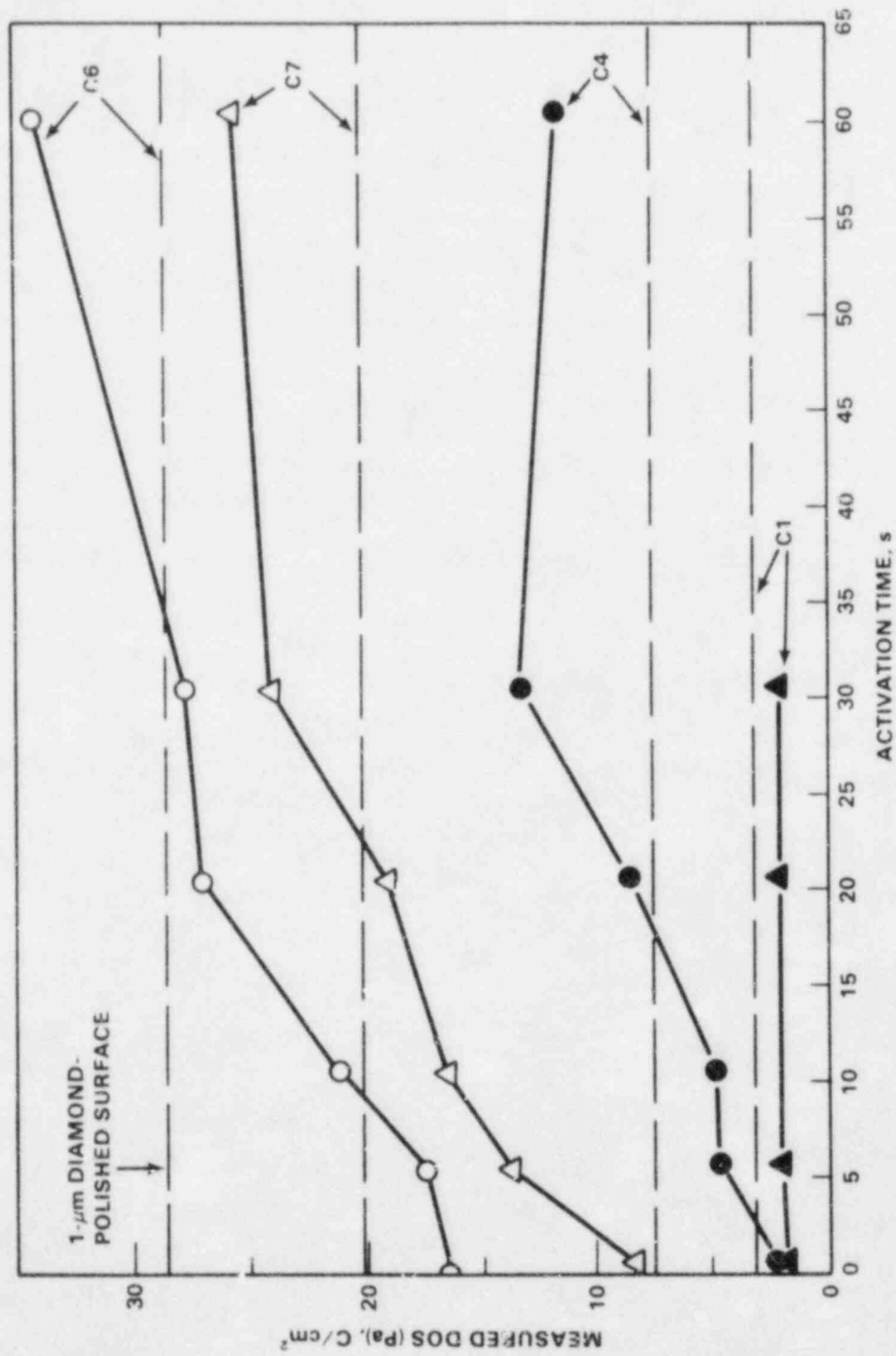
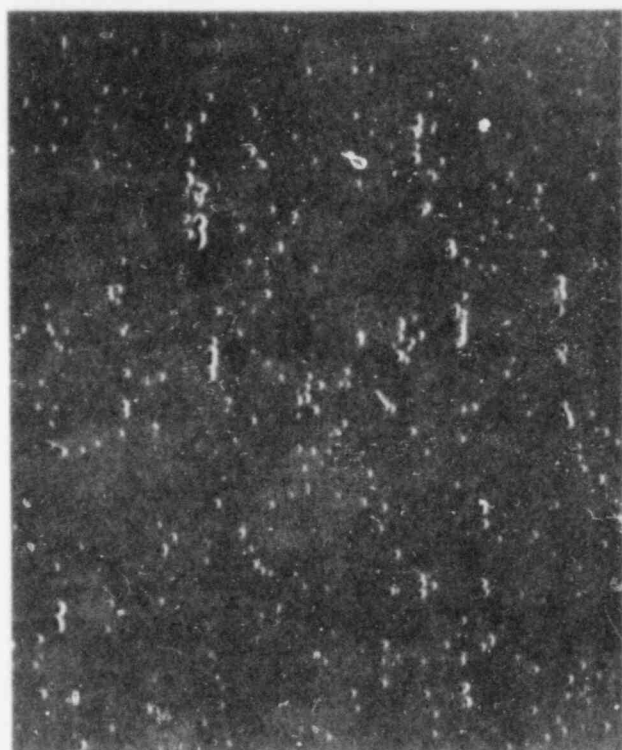


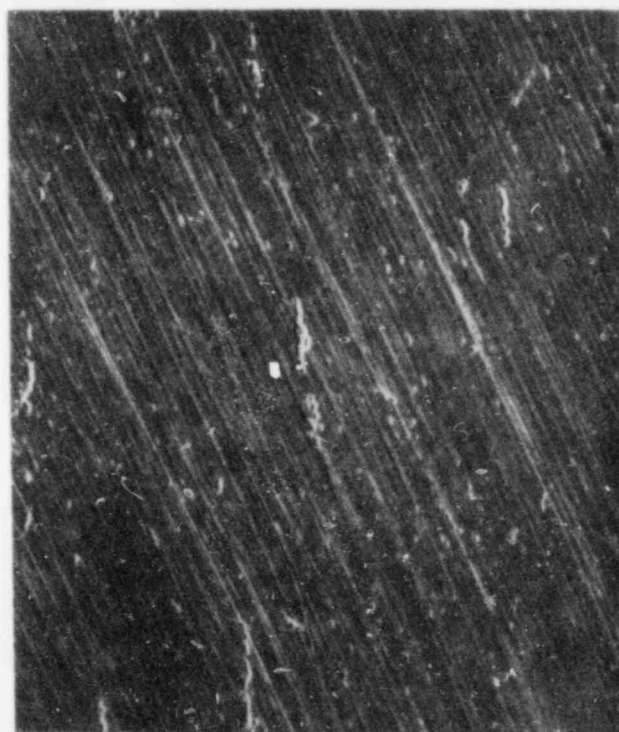
FIGURE 27. Change in EPR Measurement as a Function of Surface Activation Treatment Time (initial surface finish = 600 grit)



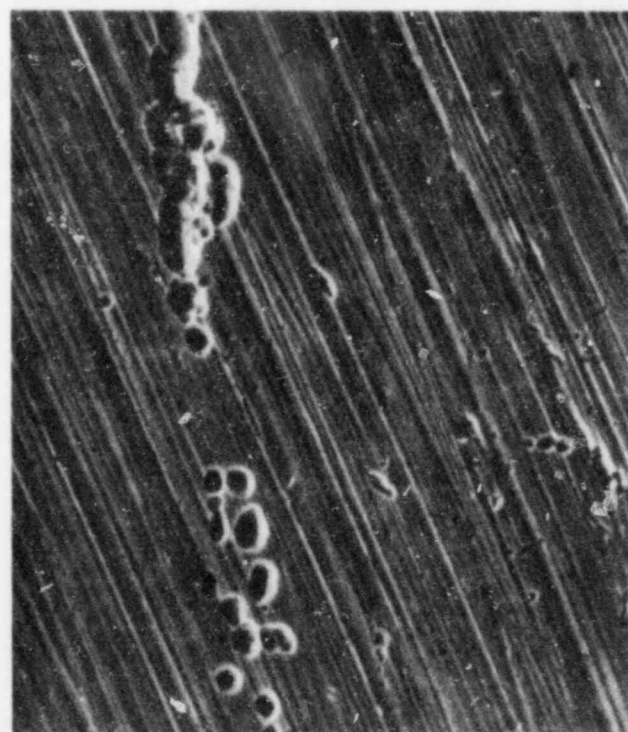
(a) 100X



(b) 500X



(c) 100X



(d) 500X

FIGURE 28. Surface Appearance After a Standard (measured EPR value 3.8, a and b) and an Activated Test (measured EPR value - 1.7, c and d) on a Furnace-Sensitized Type 304L SS

TABLE 2. Comparison of Field and Laboratory Cell EPR Tests on Furnace-Sensitized Type 304 SS

Alloy	Lab Cell			Lab Cell with MRE			Field Cell		
	E_{corr}, V	E_B, V	C/cm^2	E_{corr}, V	E_B, V	C/cm^2	E_{corr}, V	E_B, V	C/cm^2
C1	-0.492	-0.20	1.8	-0.422	-0.15	1.8	-0.436	-0.16	2.1
C4	-0.490	-0.18	9.5	-0.446	-0.14	6.5	-0.435	-0.14	5.2
C6	-0.479	-0.17	24.9	-0.438	-0.13	19.7	-0.423	-0.12	20.3
C7	-0.475	-0.11	9.2	-0.430	-0.07	9.8	-0.428	-0.08	12.0

The field cell has been used to map DOS as a function of distance from the weld metal/base metal fusion line in a high carbon Type 304 SS. The inner diameter surface from a section of a Schedule 80 pipe weld was analyzed. The surface was mechanically polished to a 600-grit finish and EPR tests were performed by activated analysis. Three probe sizes were examined:

- 0.4 cm x 0.8 cm
- 0.1 cm x 0.8 cm
- 0.05 cm x 0.8 cm.

Care was taken to ensure that the analysis area was aligned parallel to the fusion line. The results from these tests are shown in Figure 29. This particular pipe weld HAZ is severely sensitized to a distance of ~0.5 cm from the fusion line. The importance of lateral spatial resolution on measured DOS is illustrated by comparing readings at a distance of 0.3 to 0.4 cm from the fusion line. A significant increase in measured DOS is observed as the width of the analysis area is reduced from 0.4 to 0.05 cm.

STRESS CORROSION CRACKING SUSCEPTIBILITY MEASUREMENT

The primary experimental technique for evaluating the IGSCC susceptibility of SS weldments will be slow strain rate/CERTs. Preliminary design for the autoclave and loading systems has been completed. This design was based on the "pipe" autoclave/CERT systems in use at ANL. Several modifications were necessary to accommodate our different specimen design, loading requirements, monitoring capability, etc. Individual suppliers of CERT system equipment have been contacted and bids for system components have been received.

COMPOSITION EFFECTS ON SENSITIZATION: CARBON SERIES

Carbon content is the most critical compositional variable in the sensitization of stainless steels. The effect of bulk carbon content on DOS and IGSCC susceptibility will be evaluated and compared to model predictions as

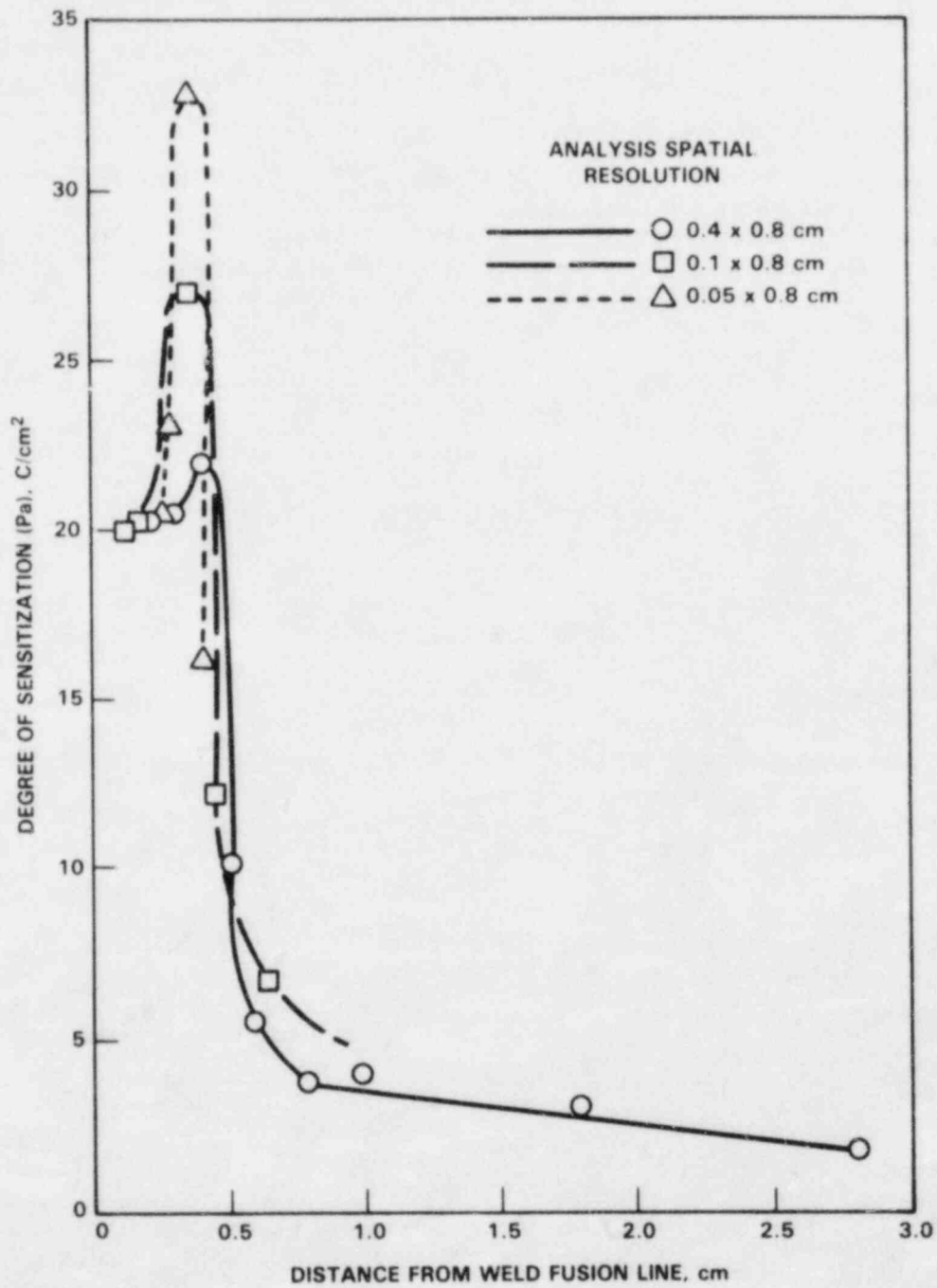


FIGURE 29. Degree of Sensitization Measurements as a Function of Distance from the Weld Fusion Line for Three Probe Sizes

described in Task III. Preliminary experiments have been initiated on a series of Type 304 SS alloys ranging in carbon content from 0.015 to 0.072 wt%. The complete chemical compositions of these alloys are listed in Table 1.

The first step in characterizing the sensitization behavior of these alloys was EPR DOS measurement of isothermally heat-treated specimens. A time/temperature matrix was selected (Table 3) to produce a range of DOS levels for each of the alloys chosen from those listed in Table 1. This overlapping range in DOS for various bulk carbon contents is needed to allow a critical comparison with model predictions and to supply specimens for EPR standards.

Measured EPR values increased with heat treatment time at 600°C and 700°C. This reflects the growth of intergranular chromium carbides and an associated chromium-depleted region. At 800°C, chromium diffusion is so rapid that a significant depletion region either does not form or is removed after short periods of heat treatment. Examples of the DOS behavior of several carbon series alloys are shown in Figure 30. Tests are continuing at the other temperatures indicated in Table 3.

The magnitude of the EPR value results primarily from dissolution of chromium-depleted regions. These regions may be associated with both inter- and intragranular precipitates. Thus, the measured value is not related solely to grain boundary chromium depletion. Problems may arise when attack is not predominately intergranular. In most cases of moderately to severely sensitized materials, surface attack is more than 90% intergranular. However, a significant amount of intragranular attack may take place on slightly sensitized materials requiring considerably more surface examination to define DOS from EPR measurements. This may be particularly important in the present program (and in service applications) where low DOS must be determined accurately. Typical surface appearance after EPR testing of sensitized Type 304 SS is shown in Figure 31. Further EPR testing and surface examination by scanning electron microscopy are planned on the carbon series materials with low DOS levels.

TABLE 3. Heat Treatment Matrix for Isothermal Testing of Carbon Series (Type 304 SS) Alloys

Temperature, °C	Time, h			
	0.1	1.0	10	100
500		X	X	X
550		X	X	X
600	X	X	X	X
650	X	X	X	X
700	X	X	X	X
800	X	X	X	

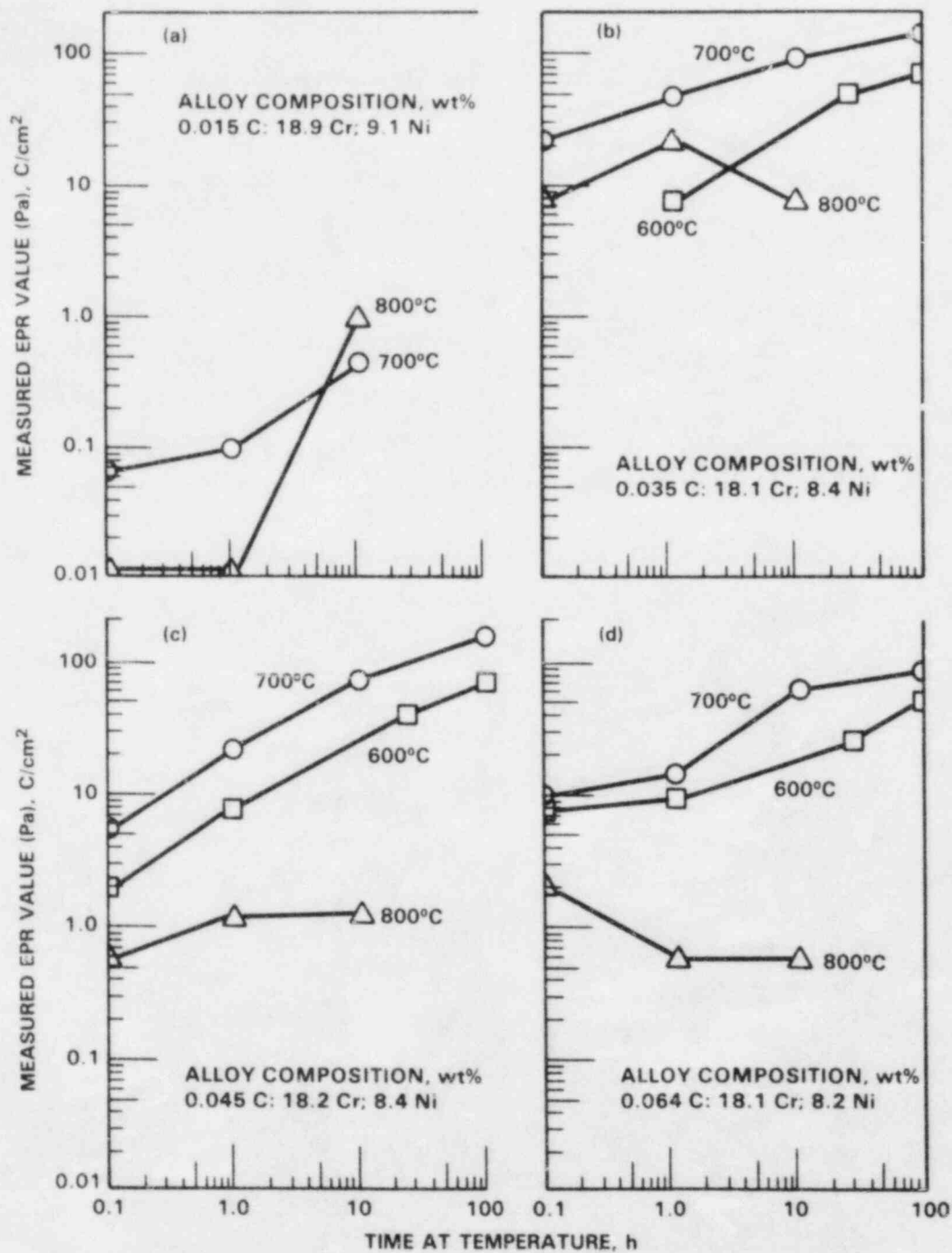
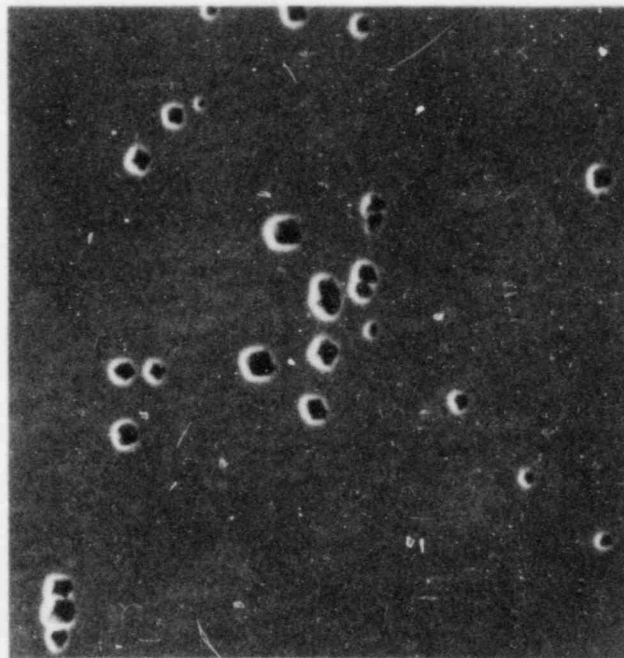


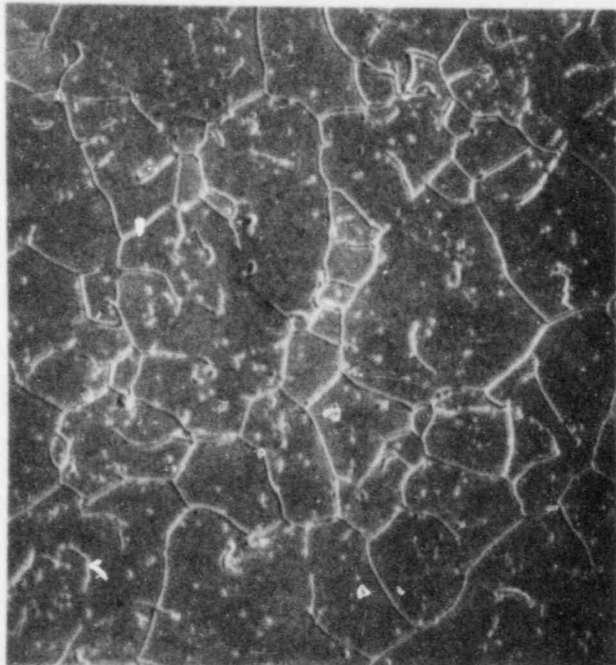
FIGURE 30. EPR Values as a Function of Isothermal Annealing Time for Three Type 304 SS Alloys of Differing Carbon Levels



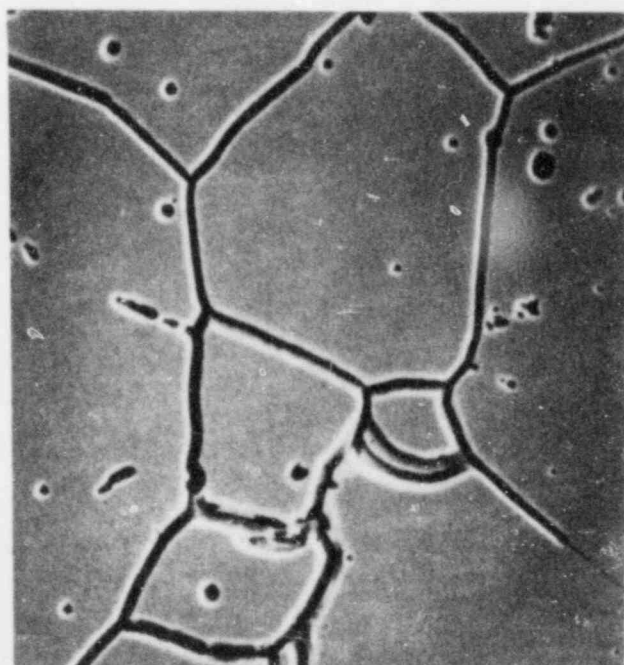
(a) 100X



(b) 500X



(c) 100X



(d) 500X

FIGURE 31. Scanning Electron Micrographs of Typical Surface Conditions after EPR Testing of Furnace-Sensitized Type 304 SS: (a) and (b) - alloy C4, measured EPR Value of 7 C/cm^2 , (c) and (d) - alloy C6, measured EPR Value of 35 C/cm^2

Several of the carbon series specimens have also been characterized by transmission and scanning transmission electron microscopy with energy dispersion x-ray spectroscopy (STEM-EDS) under a separate program. These related data allow an additional comparison among the carbon series alloys C1, C4, C6, and C7. Carbide distributions at grain boundaries (Figure 32) were found to depend on bulk carbon content for alloys with identical thermal histories. Moreover, chromium depletion as measured by STEM-EDS was in good agreement with EPR results. Correlations were made between EPR and the minimum grain boundary chromium concentration or the width of the chromium-depleted region. Examples of these correlations are shown in Figure 33. Correlations of this type are critical since predictive modeling (if based on the physical process controlling sensitization) will give the extent of chromium depletion as a first estimate of DOS and IGSCC susceptibility. No direct experimentation is planned in this area under the existing program.

INTERACTIONS WITH OTHER LABORATORIES

E. I. Husa visited E. Merrick, T. Williams and J. Lewis at TVA. Construction of several BWR reactors begun by the TVA has been terminated, leaving a large inventory of piping material, as TVA originally ordered high-carbon Type 304 SS for the primary piping systems and then ordered replacement low-carbon Type 304L SS systems before installing the original systems. This was done to decrease the potential for IGSCC. Thus, there are two primary piping systems for each terminated reactor. It was anticipated that portions of these systems could be used as piping material in this study, and a materials inventory of these systems was therefore carried out. Table 4 lists the piping that is of potential use for this study.

S. M. Bruemmer visited W. L. Clarke at GE-Vallejos to discuss the use of the EPR technique, quantification of EPR measurements, surface preparation of pipe surfaces, and correlation between EPR measurements and service experience. Clarke agreed to perform EPR tests on PNL's set of EPR standards. Discussions were also held with M. Fox of the Electric Power Research Institute (EPRI) concerning pertinent service environments for CERT/IGSCC susceptibility testing. Several documents that report and discuss water chemistry conditions in LWRs were obtained.

S. M. Bruemmer also visited W. J. Shack and J. Y. Park at ANL. Introductory program discussions were conducted. Park expressed interest in participating in mini-round robin testing on PNL's set of EPR standards. G. D. Shearer had several discussions with Park concerning CERT test system design and setup. Sketches and equipment information on the ANL pipe autoclave/CERT system were received from Shack.

R. E. Page and D. G. Atteridge visited H. D. Solomon at GE-Schenectady to discuss measurement of DOS and IGSCC in the HAZ of welds. Solomon has published extensively in the area of DOS and IGSCC and SS HAZs and has ongoing

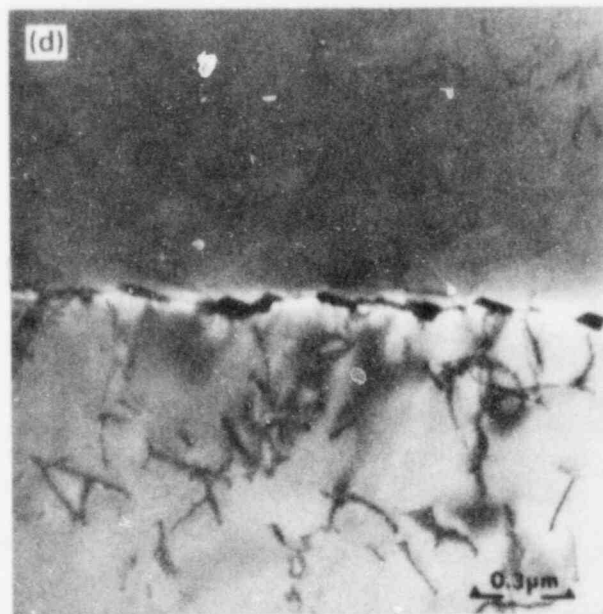
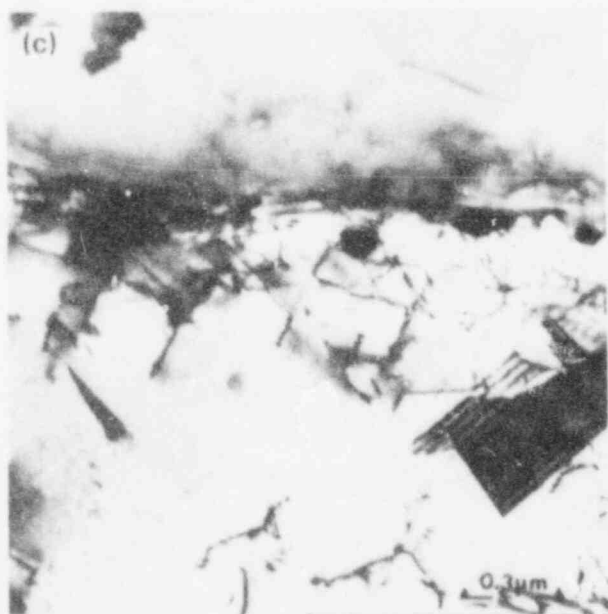
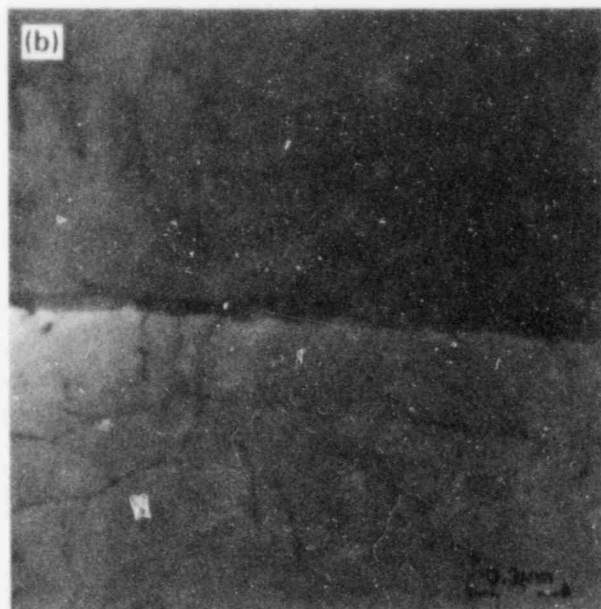
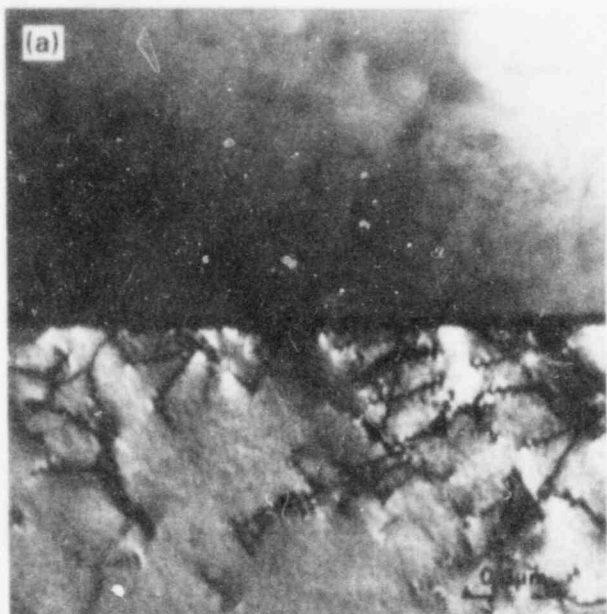


FIGURE 32. Intergranular Carbide Distributions in Four Carbon Series (Type 304 SS) Alloys After a 625°C Heat Treatment for 24 h: (a) C1, (b) C4, (c) C6, and (d) C7

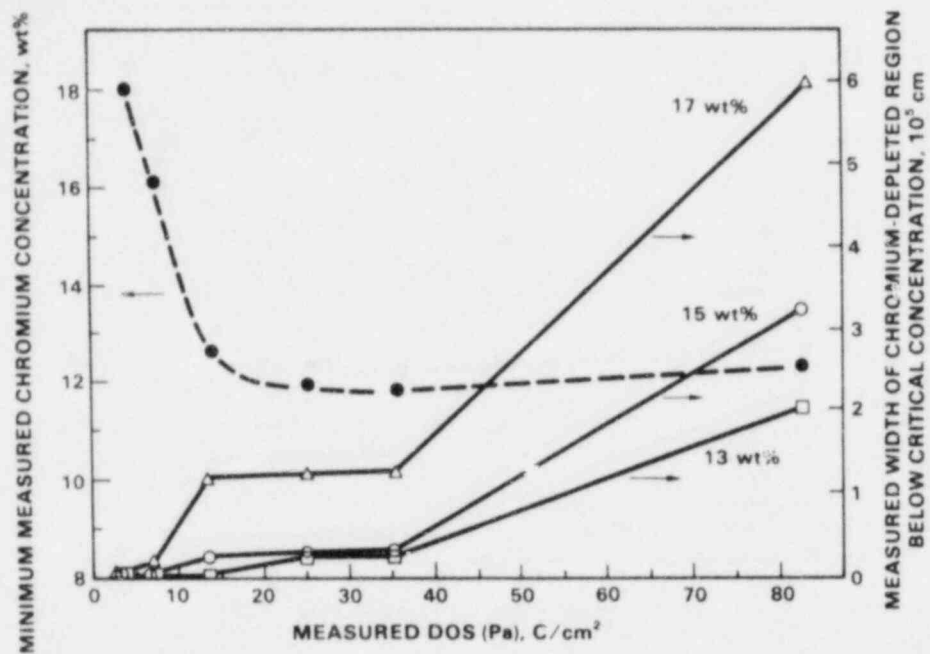


FIGURE 33. Comparison of Chromium Depletion Measured by STEM-EDS and by EPR on Furnace-Sensitized Type 304 SS Alloys. Minimum chromium contents at grain boundaries were measured with a 10-nm incident electron probe.

work in this area. He expressed interest in the project and agreed to act as a program advisor and/or perform experimental work for the program, as deemed necessary.

TABLE 4. TVA Material Selection

Heat No.	C, wt%	SS Type	Task Application	Diameter in.	Length, (a) ft
69499	0.018	316L	Task I ^(b)	24	4
69533	0.020	316L	Task I ^(c) + II	24	18
25464	0.036	304	Task II	22	21
19401	0.045	304	Task II	12	15
38462	0.047	304	Task I + II	12	30
19391	0.048	304	Task II	22	8
348530	0.057	304	Task I + II	24	20
23467	0.058	304	Task II	4	3
24205	0.060	304	Task I + II	12	15
38474	0.060	304	Task II	12	12
412364	0.61	304	Task I + II	16	37
338624	0.061	304	Task I + II	24	36
24253	0.070	304	Task II	12	12
322293	0.070	304	Task II	24	20

(a) Lengths listed assume that entire pipe sections must be obtained.

(b) Task II: Influence of Composition and Thermomechanical History on DOS and IGSCC.

(c) Task I: Weld Thermomechanical History Determination.

TASK III: IGSCC PREDICTION METHODOLOGY FROM COMPONENT-SPECIFIC THERMOMECHANICAL HISTORIES

Austenitic SS components of commercial BWRs and PWRs have experienced IGSCC in the HAZ of stainless steel welds in service. This type of cracking phenomenon, although it has been rarely observed, can result in serious component failure. Extensive research over the last several decades has defined the factors controlling the IGSCC phenomena: sensitized microstructure, tensile stress, and an aggressive environment. However, at present, IGSCC susceptibility of in-service weldments can be predicted only qualitatively.

The objective of this task is to develop and validate a methodology to quantitatively predict the IGSCC susceptibility of HAZ regions in austenitic SS weldments. The basic methodology will include:

- DOS prediction from material composition and initial condition
- TM history prediction from welding and/or repair welding parameters
- DOS prediction from TM history
- IGSCC susceptibility prediction from DOS measurements.

Each of these steps will be assessed by direct comparison to the experimental data base generated in Tasks I and II. Existing models will be evaluated, modified (where appropriate), and combined.

DEGREE OF SENSITIZATION PREDICTION: EFFECT OF COMPOSITION

A literature review of existing models that correlate alloy composition to DOS and/or IGSCC has been initiated. Several of these models have been used to evaluate the carbon series alloys discussed previously (see Table 1). A brief description of each model is given below. Predictions are then correlated to experimental EPR measurements of DOS after selected isothermal heat treatments.

Cihal² suggested that alloy composition effects on IGSCC could be understood by considering "effective" chromium and carbon concentrations, which are defined as:

$$Cr^* = Cr + 1.7 Mo$$

$$C^* = C + 0.002 [Ni - 10]$$

The constants in the equations above were determined empirically. Effective concentrations can then be used to define a "composite" chromium value (K) which indicates equivalent IGSCC susceptibility:

$$K = Cr^* - 100C^*$$

These parameters have been used graphically for material evaluation as shown in Figure 34. Equivalent IGSCC susceptibility is predicted for compositions lying along a line of the slope depicted in this figure. Increased susceptibility is predicted for compositions below this line. Predictions for the carbon series alloys are shown in Figure 34 and in Table 5. Decreasing composite chromium values, and therefore increasing IGSCC susceptibility, are predicted for alloys in the following order: C1, C2, C3, C4, C5, C6, C7.

A more complete and thermodynamically-based method for determining the effect of individual alloying elements on the composite chromium value was proposed by Fullman.³ Thermodynamic data on Fe-Cr-Ni-(M)-C interactions were used to assess the Cr concentration in equilibrium with an $M_{23}C_6$ -type carbide as a function of alloy composition. An equation for the composite Cr value, based on Fullman's calculations at 600°C, can be written as:

$$K = Cr + 0.15 Mn + 1.42 Mo + 0.15 W - 0.2 Co + 0.2 Cu \\ - 0.2 Ni - 0.3 Al - 0.2 Si + Ti + 0.75V - 11.3 \\ (\log C - \log 0.04) - 4$$

The final method for estimating the composite Cr value listed in Table 5 (referred to as an "effective" Cr content) was presented by Briant et al.^{4,5} It is a simplified version of the other two, with coefficients based on empirical correlations between Types 304 and 316 SS alloys. The composite Cr value is defined as

$$K = Cr^{eff} = Cr - 0.18 Ni - 100 C$$

Although the magnitude of the composite Cr values differ among the three equations, the alloy order of increasing IGSCC susceptibility is the same.

The difficulty of applying these methods to predict compositional effects on DOS is illustrated in Figures 35 and 36, in which EPR-measured DOS is correlated with predicted composite Cr values for several of the carbon series alloys. After a 625°C/24 h heat treatment, a reasonable correlation between decreasing composite Cr and increasing DOS is observed (Figure 35). However, at other time and temperature combinations, such as 700°C for 10 h (Figure 36), moderate values of composite Cr show the higher sensitization levels. This is, in part, to be expected since DOS at any time depends not only on carbide thermodynamics but also on the kinetics of Cr diffusion. Thus, composite Cr values should best correlate with maximum DOS for a given composition.

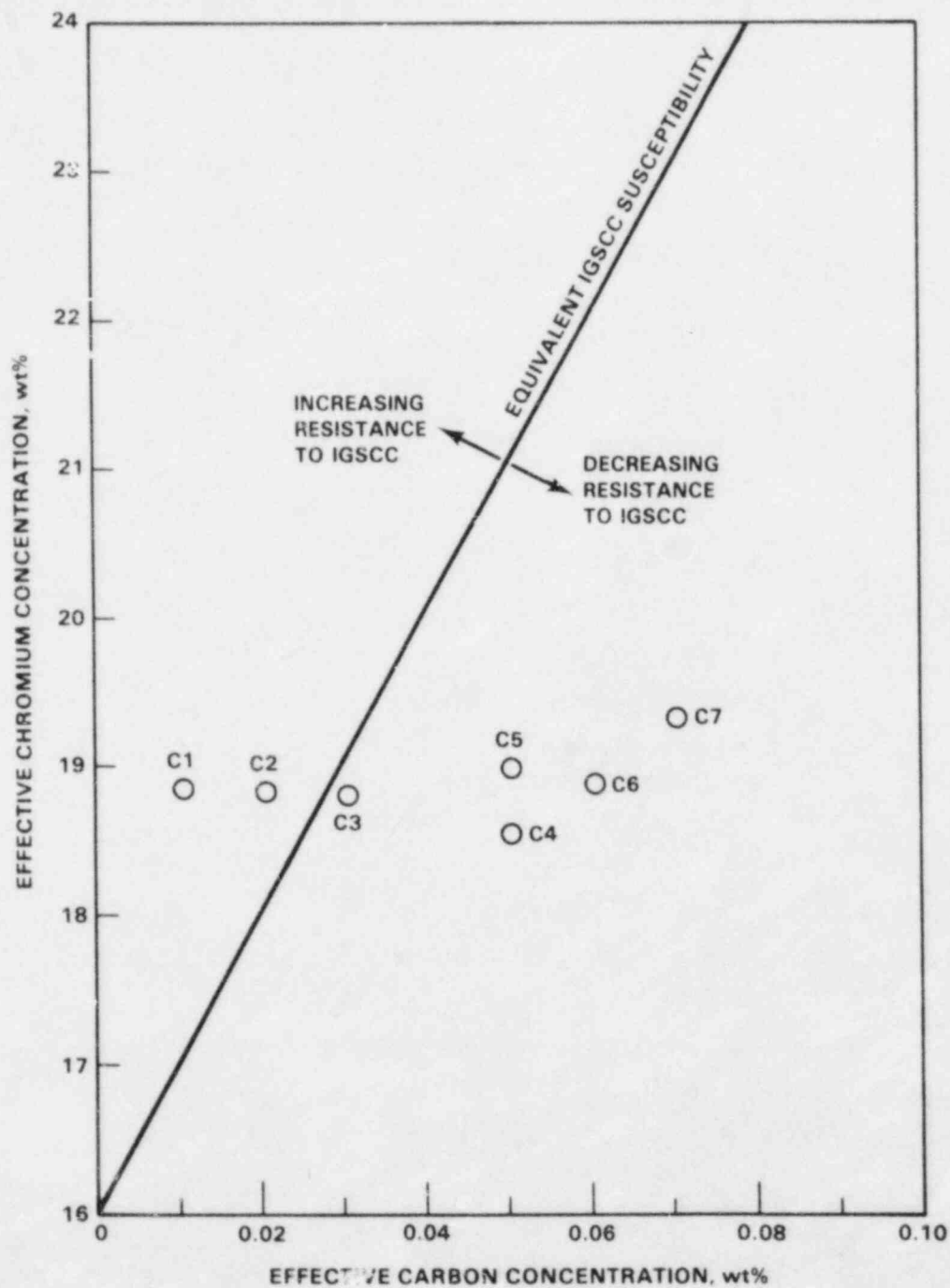


FIGURE 34. Cihal Plot Indicating Relative IGSCC Susceptibility for Carbon Series Alloys. Compositions along a line of a slope as the one shown have equivalent IGSCC susceptibility.

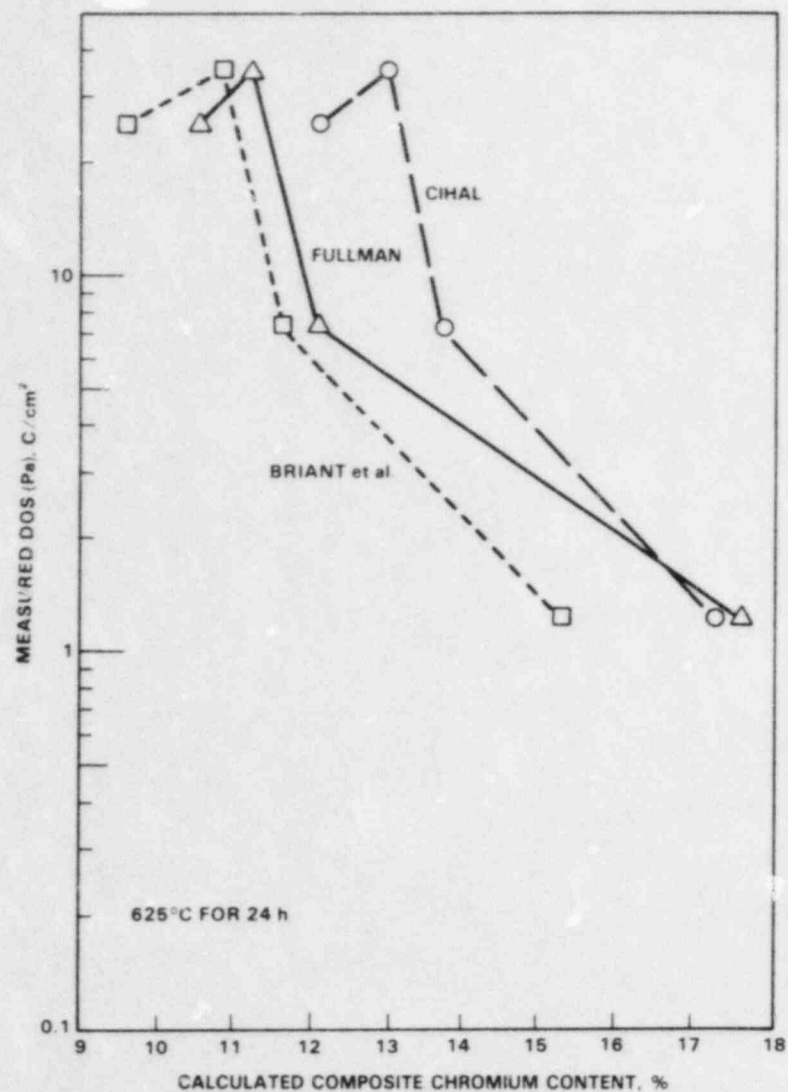


FIGURE 35. Comparison of EPR-Measured Degree of Sensitization to the Predicted Composite Chromium Content from Composition Models; 625°C for 24 h.

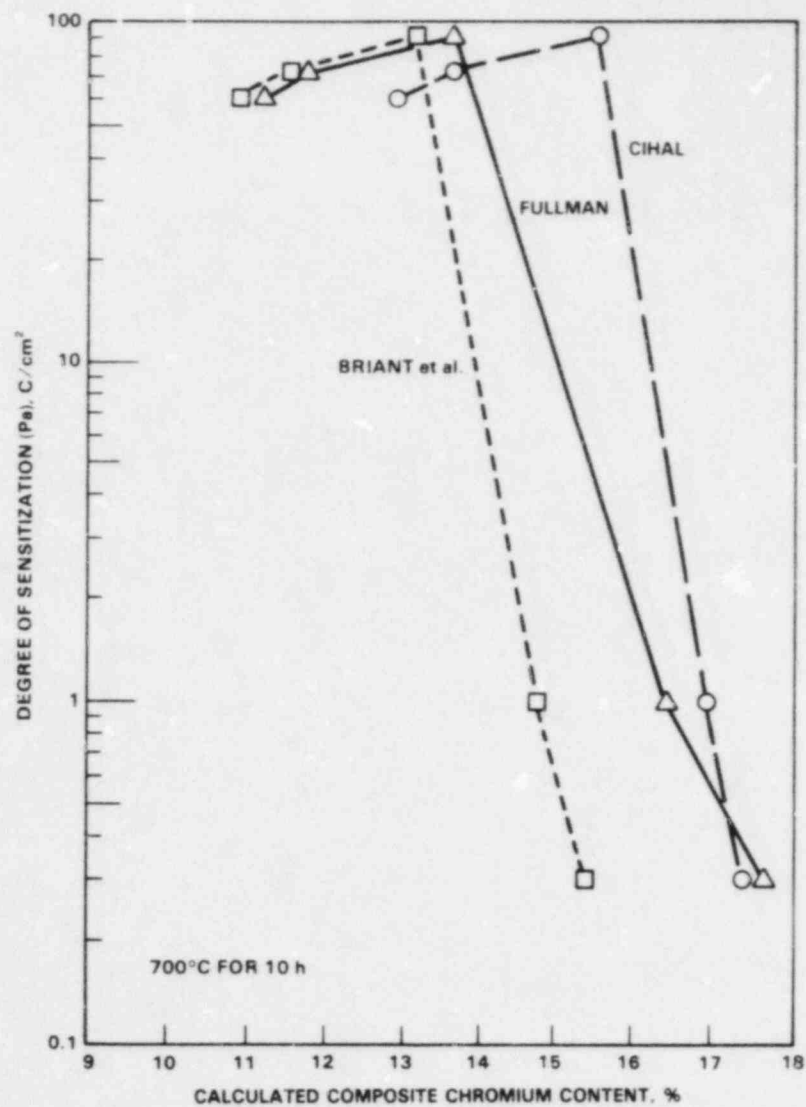


FIGURE 36. Comparison of EPR-Measured Degree of Sensitization to the Predicted Composite Chromium Content from Composition Models; 700°C for 10 h.

TABLE 5. Comparison of Model Predictions for Chromium Equivalent Parameters of Carbon Series Alloys

Alloy	Cihal		Kcr	Fullman	Briant
	Cr*	C*		Kcr	Kcr
C1	18.79	0.013	17.41	17.70	15.35
C2	18.77	0.018	16.97	16.51	14.75
C3	18.74	0.032	15.59	13.90	13.27
C4	18.48	0.042	13.83	11.89	11.67
C5	18.93	0.048	14.15	12.22	12.03
C6	18.82	0.059	13.07	11.30	10.91
C7	19.26	0.071	12.20	10.60	9.65

DEGREE OF SENSITIZATION PREDICTION: KINETICS OF CHROMIUM DEPLETION

A kinetic model for the development of a Cr-depleted region has been set up based on the work of Stawstrom and Hillert⁶ and of Tedmon et al.⁷ The width of the depleted zone (i.e., zone where chromium content is below some critical value) can be estimated by the equation:

$$W = 2 \sqrt{Dt} \frac{(C_c - C_e)}{(C_o - C_e)}$$

where

- D = Cr diffusion coefficient at some temperature T
- t = time at temperature
- C_c = critical C_r concentration
- C_e = equilibrium Cr concentration at the grain boundary
- C_o = concentration of the bulk alloy.

Critical Cr concentrations from 13 at.% to 17 at.% have been used to "fit" experimental data.⁶⁻⁷

Preliminary comparisons have been made between EPR-measured DOS and the predicted width of the Cr-depleted zone. A particularly good example is shown in Figure 37 for alloy C4 at 700°C. This curve illustrates the type of prediction that is being attempted and its evaluation by experimental DOS measurement.

INTERACTIONS WITH OTHER LABORATORIES

E. F. Rybicki, University of Tulsa, agreed to attempt to use his finite element pipe welding residual strain prediction model to predict TM histories during welding.

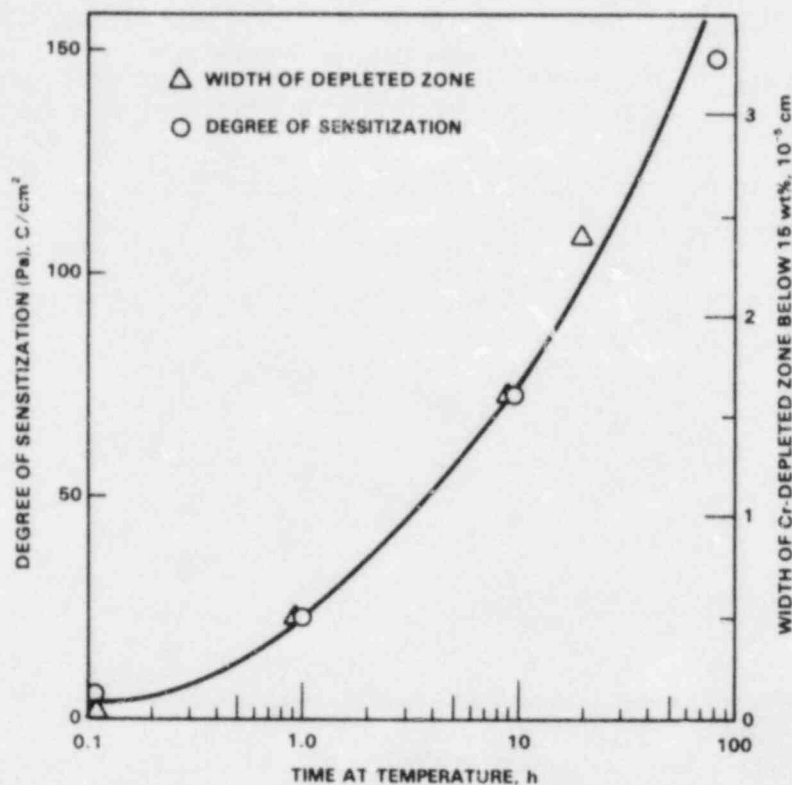


FIGURE 37. Correlation Between the EPR-Measured Degree of Sensitization and the Predicted Width of the Chromium-Depleted Region at Grain Boundaries as a Function of Heat Treatment Time at 700°C

FUTURE RESEARCH PLANS

The basis for future research is the collection of TM-DOS data during SS pipe welds/repairs. This data will be used to develop a method for predicting the DOS in the HAZ of a SS weld/repair, and to develop realistic weld/repair simulation cycles that will be applied to a variety of SS compositions. The DOS results from these latter specimens will be used in the development of the DOS prediction models.

Both weld/repair and simulation specimens will be submitted to constant extension rate tests (CERTs) to develop an empirically based correlation between DOS and IGSCC susceptibility. This correlation will allow prediction of the weld/repair resistance to IGSCC during the life of the component, based on the DOS prediction for a given nuclear reactor weld/repair.

REFERENCES

1. Clarke, W. L. April 1981. EPR Method for the Detection of Sensitization in Stainless Steels. NUREG/CR-1095, General Electric Company, Pleasanton, California.
2. Cihal, V. 1969. "Intergranular Corrosion of Cr-Ni Stainless Steels." Presented at Unieux Conference, May 5, 1969.
3. Fullman, R. L. August 1981. A Thermodynamic Model of the Effect of Composition on the Susceptibility of Austenitic Stainless Steel to Intergranular Stress Corrosion Cracking. Report 81CRD187, General Electric Company, Corporate Research and Development, Schenectady, New York.
4. Briant, C. L., et al. September 1982. "Sensitization of Austenitic Stainless Steel, I. Controlled Purity Alloys." Corrosion 38(9):468.
5. Mulford, R. A., E. L. Hall, and C. L. Briant. April 1983. "Sensitization of Austenitic Stainless Steel, II. Commercial Purity Alloys." Corrosion 39(4):132.
6. Stawström, C., and M. Hillert. January 1969. "An Improved Depleted-Zone Theory of Intergranular Corrosion of 18-8 Stainless Steel." J. Iron Steel Inst. 207:77.
7. Tedmon, C. S., Jr., et al. 1971. "Intergranular Corrosion in Austenitic Stainless Steel." J. Electrochemical Soc. 188(2):192.

DISTRIBUTION

No. of
Copies

No. of
Copies

OFFSITE

	3	E. Merrick Division of Engineering Design Tennessee Valley Authority 400 Commerce Avenue W10-B119C-K Knoxville, TN 37902
	3	W. J. Shack Materials Science Division Argonne National Laboratory 9700 South Cass Avenue Argonne, IL 60439
2		DOE Technical Information Center
5	3	J. Muscara Materials Engineering Technology Division Nuclear Regulatory Commission Mail Stop 565UNL Washington, DC 20555
		E. F. Rybicki Mechanical Engineering Dept. University of Tulsa 600-South College Ave. Tulsa, OK 74104
		H. D. Solomon Materials Characterization Laboratory Corporate Research & Development General Electric Company P.O. Box 8 Schenectady, NY 12301
		W. J. Childs Nuclear Power Division Electric Power Research Institute 3412 Hillview Avenue Palo Alto, CA 94304
		K. W. Mahin Lawrence Livermore Laboratory University of California P.O. Box 808 L-2A Livermore, CA 94550
		W. E. Wood Oregon Graduate Center 19600 N.W. Walker Road Beaverton, OR 97006

No. of
Copies

ONSITE

J. F. Key
Fuels & Materials Division
EG&G Idaho, Inc.
P.O. Box 1625
Idaho Falls, ID 83401

R. Horn
General Electric Company
Nuclear Energy Engineering
Division
175 Curtner Ave.
San Jose, CA 95125

No. of
Copies

50 Pacific Northwest Laboratory

W. E. Anderson
D. G. Atteridge (10)
S. M. Bruemmer (10)
L. A. Charlot
R. A. Clark
C. R. Hann
P. E. Hart
E. I. Husa
R. S. Kemper (2)
R. F. Klein
B. Norton
R. E. Page (10)
J. P. Pilger
F. A. Simonen
P. L. Whiting
Publishing Coordination (2)
Technical Information (5)

NRC FORM 335 U.S. NUCLEAR REGULATORY COMMISSION BIBLIOGRAPHIC DATA SHEET		1. REPORT NUMBER (As assigned by DDC) NUREG/CR-361 PNL-4941	
4. TITLE AND SUBTITLE (Add Volume No., if appropriate) Evaluation and Acceptance of Welded and Repair-Welded Stainless Steel for LWR Service: Annual Report for 1983		2. (Leave blank)	
7. AUTHOR(S) D.G. Atteridge, S.M. Bruemmer, R.E. Page		3. RECIPIENT'S ACCESSION NO.	
9. PERFORMING ORGANIZATION NAME AND MAILING ADDRESS (Include Zip Code) Pacific Northwest Laboratory P. O. Box 999 Richland, Washington 99352		5. DATE REPORT COMPLETED MONTH YEAR September 1983	
12. SPONSORING ORGANIZATION NAME AND MAILING ADDRESS (Include Zip Code) Division of Engineering Technology Office of Nuclear Regulatory Research U.S. Nuclear Regulatory Commission Washington, DC 20555		DATE REPORT ISSUED MONTH YEAR June 1984	
13. TYPE OF REPORT Annual		6. (Leave blank)	
15. SUPPLEMENTARY NOTES		8. (Leave blank)	
16. ABSTRACT Pacific Northwest Laboratory (PNL), under a program sponsored by the Division of Engineering Technology of the U.S. Nuclear Regulatory Commission (NRC), is conducting a program to determine a method for evaluating the acceptance of welded and repair-welded stainless steel (SS) piping for light-water reactor (LWR) service. Validated models, based on experimental data, will be developed to predict the degree of sensitization (DOS) and the intergranular stress corrosion cracking (IGSCC) susceptibility in the heat affected zone (HAZ) of the SS weldments. IGSCC is caused by a combination of a sensitized microstructure, an aggressive environment, and tensile stress. Control of any of these three factors can eliminate IGSCC in most practical situations. This program will measure and model the development of a sensitized microstructure as it pertains to welded and repair-welded SS pipe. An empirical correlation between a material's DOS and its susceptibility to IGSCC will be determined using constant extension rate tests (CERTs). The successful completion of these tasks will result in a method for assessing the effects of welding/repairing parameters on the IGSCC susceptibility of component-specific nuclear reactor welds/repairs.		10. PROJECT TASK/WORK UNIT NO.	
17. KEY WORDS AND DOCUMENT ANALYSIS Austenitic stainless steel Intergranular stress corrosion cracking Heat affected zone Degree of sensitization		11. FIN NO. FIN B2449	
17b. IDENTIFIERS: OPEN ENDED TERMS		14. (Leave blank)	
18. AVAILABILITY STATEMENT Unlimited		19. SECURITY CLASS (This report) Unlimited	
20. SECURITY CLASS (This page) Unlimited		21. NO. OF PAGES 5	

UNITED STATES
NUCLEAR REGULATORY COMMISSION
WASHINGTON, D.C. 20555

OFFICIAL BUSINESS
PENALTY FOR PRIVATE USE, \$300

FOURTH CLASS MAIL
POSTAGE & FEES PAID
USNRC
WASH D.C.
PERMIT No. 667

NUREG/CR-3613

120555078877 1 JAN 1985
US NRC
ADM-DIV OF TIDC
POLICY & PUB MGT BR-PDR NUREG
W-501
WASHINGTON DC 20555

EVALUATION AND ACCEPTANCE OF WELDED AND REPAIR-WELDED
STAINLESS STEEL FOR LWR SERVICE

JUNE 1984